CHAPTER 2 PHYSICAL AND OCEANOGRAPHIC SETTING

Julie Kellner, John Christensen, Randy Clark, Chris Caldow, Michael Coyne

2.1 PHYSICAL ENVIRONMENT AND GEOLOGY

The following sections provide a brief overview of the physical and oceanographic environment for the region of interest. Much of the material is excerpted or summarized from the *Draft Environmental Impact Statement for Channel Islands Marine Sanctuary* (CINMS, 2000) and *Ecological Linkages: Marine and Estuarine Ecosystems of Central and Northern California* (Airamé *et al*., 2003a) reports. This section describes the physical, climatic and oceanographic setting near the Channel Islands and supplements the subsequent analytical chapters which provide spatially-articulated assessments of both dynamic and static habitats of the region.

Figure 2.1.1 shows the geologic and bathymetric features for the region of interest. The four northern Channel Islands (San Miguel, Santa Rosa, Santa Cruz and Anacapa) parallel the east-west trend of the coast, and vary from 20 to 40 km offshore. Santa Barbara Island lies about 64 km south of Point Mugu, California. These islands are all located within a unique oceanographic region known as the Continental Borderland (Norris and Webb, 1990).

The Continental Borderland is located offshore of California between Point Conception and Punta Banda in Baja California (Mexico). Continued large-scale overriding of the North American Plate by the Pacific Plate in southern California caused movement along the San Andreas Fault System (Dailey *et al*., 1993). The Continental Borderland, with its wide shelf (up to 483 km seaward) and series of laterally shifted blocks, resulted from this movement (Dailey *et al*., 1993). Unlike most wide continental shelves that consist of gently sloping platforms interrupted by low banks and occasional canyons, the Continental Borderland is a region of basins and elevated ridges. The Channel Islands are the portions of the ridges that rise above sea level. The highest point in the Channel Islands is Picacho Diablo on Santa Cruz Island, with an elevation of 747 m. The seaward edge of the Continental Borderland is the Patton Escarpment, a true continental slope that descends 4,000 m to the deep ocean floor (Norris and Webb, 1990). Basin slopes account for 63% (49,753 km^2) of the borderlands area (Norris and Webb, 1990). Basin floors represent 17% of the total area (13,260 km^2), while the islands only comprise 1.1% of the total (880

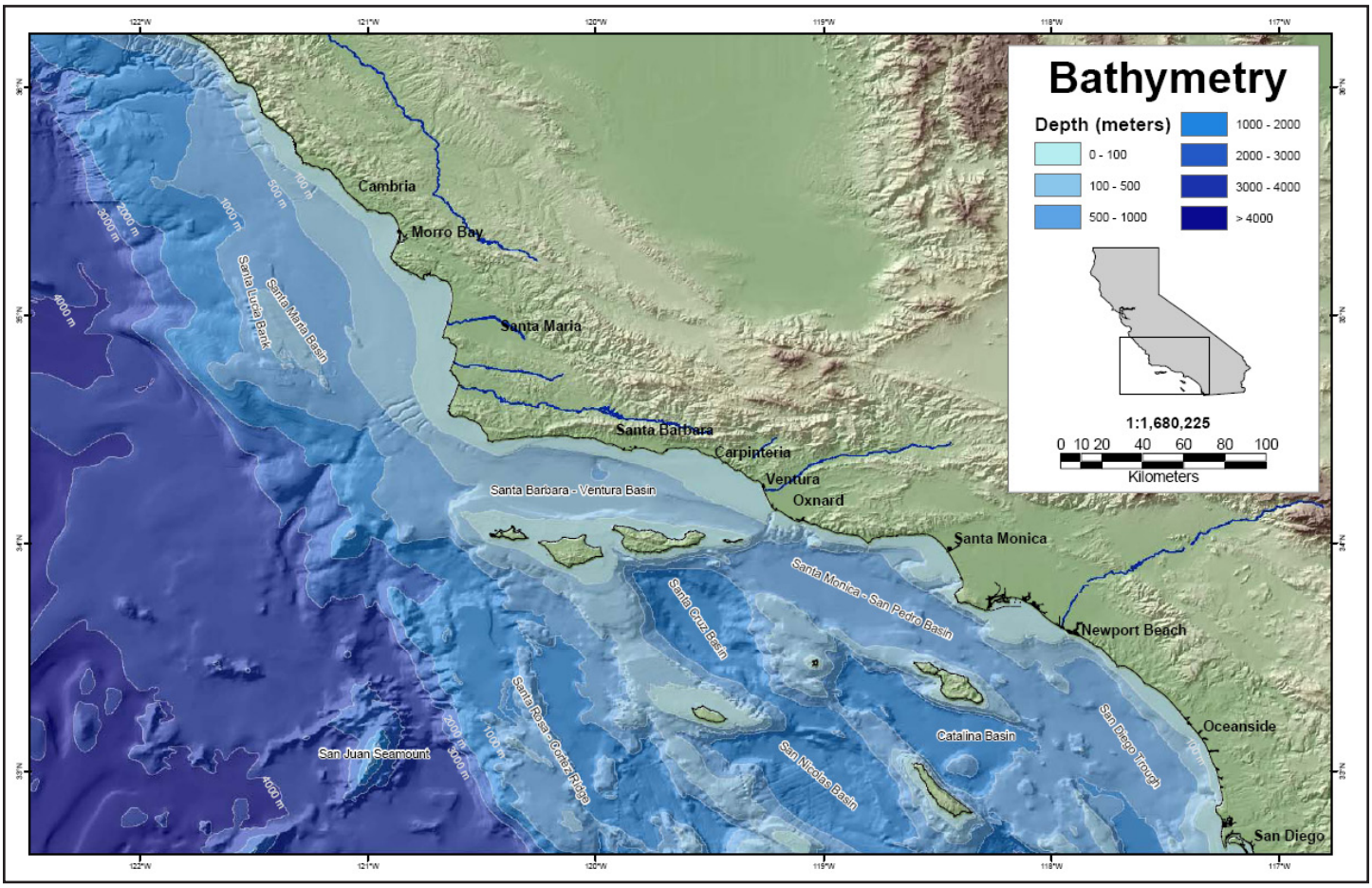

Figure 2.1.1. Bathymetric and geologic features of the region of interest.

km^2). The basins nearest the mainland have the shallowest depths, flattest floors and thickest sediment fills and range in depth from 500 to 2,500 m.

The Santa Barbara-Ventura Basin, oriented east-west in parallel with the coastline and the islands, lies between the islands and the mainland, and is approximately 500 m deep, 297 km long, up to 88 km wide, and approximately 13,000 km^2 in area. This basin is located within the Transverse Ranges Province, which also includes the Santa Ynez and Santa Monica Mountains, and the Channel Islands. The submerged portion of the Santa Barbara-Ventura Basin, an area of 5,179 km^2 and approximately 97 km in length from Point Conception to Port Hueneme, is commonly referred to as the Santa Barbara Channel. The western entrance to the channel is approximately 97 km wide with a sill depth of about 450 m, whereas the Anacapa Passage, the eastern entrance to the channel, is more limited with a width of 19 km and a shallower sill depth of 200 m (Dever, 2004). The remaining basins in the Southern California Bight, such as the Santa Cruz Basin to the south of the northern Channel Islands and the Santa Monica-San Pedro Basin to the southeast, trend northwest-southeast.

North of the Continental Borderland, the offshore Santa Maria Basin abuts the Santa Barbara-Ventura Basin at a location known as the “Amberjack High”. This basin extends north-northwest from Point Conception to Point Buchon and is approximately 160 km in length, 16 to 80 km wide, and approximately 7,769 km^2 in size. It is bounded on the east by the Hosgri and related fault zones, and on the west by Santa Lucia Bank.

There are at least 32 submarine canyons in the Continental Borderlands. Along the mainland coast are six prominent canyons that are thought to be related to the modern shoreline. Other coastal canyons appear to be related to the shoreline and lower sea levels during the Ice Age that ended approximately 12,000 years ago (Norris and Web, 1990). There are also canyons cut into offshore basins in the region (Dailey *et al*., 1993).

2.2 CLIMATE AND METEOROLOGY

Santa Barbara County has a Mediterranean climate characterized by mild winters, when most rainfall occurs, and warm, dry summers. The regional climate is dominated by a strong and persistent high-pressure system that frequently lies off the Pacific coast (generally referred to as the Pacific High). The Pacific High shifts northward or southward in response to seasonal changes or the presence of cyclonic storms. In its usual position to the west of Santa Barbara County, the Pacific High produces an elevated temperature inversion. Coastal areas are characterized by early morning southeast winds, which generally shift to northwest later in the day. Transport of cool, humid marine air onshore by these northwest winds causes frequent fog and low clouds near the coast, particularly during night and morning hours in the late spring and early summer months.

The terrain around Point Conception, combined with the change in orientation of the coastline from north-south to east-west, can cause counterclockwise circulation (eddies) to form east of the point. These eddies fluctuate from time to time and place to place, leading to highly variable winds along the southern coastal strip. Point Conception also marks the change in the prevailing surface winds from northwesterly to southwesterly.

During the fall and winter months, the region is subject to Santa Ana winds, which are warm, dry, strong, and gusty winds that blow northeasterly from the inland desert basins through the mountain valleys and out to sea. Wind speeds associated with Santa Ana conditions are generally 24 to 32 km/h, although they can reach speeds in excess of 96 km/h.

2.3 PHYSICAL OCEANOGRAPHY

The oceanography in the Study Area is closely tied to the processes of the California Current System which forms the eastern portion of the clockwise North Pacific Subtropical Gyre and extends 3,000 km from the Straight of Juan de Fuca (Vancouver Island) to Baja California Sur. The California Current is predominantly a wind-driven system and encompasses three major currents: the equatorward California Current, the poleward California Undercurrent and the poleward Southern California Countercurrent (which occasionally combines with the Davidson Current north of Point Conception).

In the Study Area, currents in the Santa Barbara Channel include patterns of warm, saline water from the Southern California Countercurrent and the colder water from the California Current. Upwelling often occurs where these water masses meet near the headlands of Point Arguello and Point Conception, as well as along much

of the California coast, depending on the season. Upwelling plumes expand southward from headlands and frequently enter the Santa Barbara Channel on the southern side of the western mouth (Atkinson *et al*., 1986). There can be a channelwide response to upwelling north of Point Conception (Auad *et al*., 1998). Oceanographic thermal fronts are abundant in the Santa Barbara Channel and form as a consequence of upwelling and current shear between the two primary currents (Harms and Winant, 1998).

Offshore Ocean Currents

Offshore circulation in the Study Area is dynamic and results from the interaction of large-scale ocean currents, local geography, and the unique basin and ridge topography of the ocean bottom in the Southern California Bight. The prevailing wind system of the North Pacific Ocean is the mid-latitude Westerlies, a belt of winds that blow from west to east between 30°N and 60°N. These westerly winds create the North Pacific Current that pushes water away from Asia towards the west coast of North America. As this trans-Pacific flow converges toward the North American coastline, it is deflected equatorward forming the eastern boundary of the California Current. This surface current is dominant year round, and appears as a slow, broad southeastern flow that transports cool, fresh, nutrient and oxygen-rich subarctic water equatorward. The California Current extends from the shelfbreak to an offshore distance of approximately 1,000 km, with strongest speeds at the surface and extending to at least 500 m in depth (Hickey, 1998), while the inshore section of the current is limited to the upper 200 m over the continental slope (Hickey, 1979). North of Point Conception, the core lies about 100-200 km from the coast, with maximum equatorward velocities of 5-10 cm/s (Chelton, 1984). South of Point Conception, the core of the California Current flows further from the coast between 300-400 km offshore (Lynn and Simpson, 1987) with average speeds generally less than 25 cm/s (Reid and Schwatzlozse, 1962). Seasonal maxima in current speeds occurs in the summer to early fall.

South of Point Conception, a portion of the California Current turns shoreward into the Southern California Bight both north and south of the Channel Islands. Near San Diego, a larger branch of the California Current bends poleward into the SCB, where it is known as the Southern California Countercurrent. This nearshore countercurrent dominates the mean water circulation in the Southern California Bight during summer and winter (Hickey, 1993) at poleward speeds of 10-20 cm/s (Oey, 1999). Huyer *et al*. (1989), Harms and Winant (1998) and Oey (1999) have suggested that this countercurrent is caused by equatorward weakening of the wind curl south of Point Conception.

The Southern California Countercurrent draws warmer water from the south and forces the water northwest through the southern Channel Islands and the Santa Barbara Channel (Dailey *et al*.,1993). Additionally, some of the countercurrent is deflected west into the California Current south of the northern Channel Islands, resulting in a seasonal counterclockwise gyre in the Southern California Bight called the Southern California Eddy (Lynn and Simpson, 1987, Hickey, 2000). In spring, when the countercurrent is at its minimum northward flow, equatorward surface flow prevails in the Southern California Bight (Hickey 1993). Hickey (1979) suggested that the Southern California Countercurrent may combine with the poleward Davidson Current north of Point Conception, the latter having peak flows during winter.

Underlying the California Current and the Southern California Countercurrent is a subsurface flow called the California Undercurrent, a narrow (10-40 km) poleward flow that extends the length of the coastline from Baja California to at least 50°N (Hickey, 1998). Originating in the eastern equatorial Pacific, the California Undercurrent can be characterized by a warm, saline, oxygen and nutrient-poor signature (Neander, 2001). Peak northward speeds of 30-50 cm/s usually occur in summer to early fall, being stronger at depths 100-300 m, and can be continuous over distances of more than 400 km along the continental slope (Collins *et al*., 1996; Pierce *et al*., 2000) or can break into separating, mesoscale jets (Cornuelle *et al*., 2000; Barth *et al*., 2000).

Circulation in the Study Area is also influenced by coastal upwelling, a process regulated by prevailing winds and the orientation of the coastline. In the northern hemisphere, Ekman transport causes surface water to move ~45 degrees to the right of the wind direction. Where surface water is pushed away from the coastline, deeper nutrient rich water rises to the surface creating an upwelling current. Along the north-south oriented coast of California, winds blowing from the north move surface water westward, away from the coastline, creating upwelling currents that bring colder water to the surface (San Francisco State University, 2000). North of Santa Cruz (>37°N), a strong seasonal contrast in winds results in favorable upwelling conditions in summer contrasted by downwelling during winter storms (Strub and James, 2000). From 35-37°N, modest storm activity results in monthly mean winds that remain upwelling-favorable year round (Strub and James, 2000). In contrast, upwell-

ing is rare along the mainland coast of the Santa Barbara Channel because the headlands at Point Conception shelter the east-west oriented channel from the strong northwesterly winds that generate upwelling (Love *et al*., 1999). Point Conception is the southernmost major upwelling center on the west coast of the United States, and marks a transition zone between cool surface waters to the north and warm waters to the south (Love *et al*., 1999). However, upwelled water from regions north of the Bight appears to enter the western end of the Santa Barbara Channel and move eastward along its southern boundary (Hickey, 2000).

The currents and upwelling effects, with their varying water temperatures, create at least three climatic/habitat zones in the Santa Barbara Channel and the surrounding region. Waters north of Point Conception and offshore and south of the Channel Islands are cool, and have biotic assemblages characteristic of northern and central California (Oregonian Biogeographic Province) (Airamé *et al*., 2003b). San Miguel Island is primarily influenced by the cool water of the California Current, and also lies in the Oregonian Biogeographic Province. The warm waters of the California Countercurrent dominate the Santa Barbara Channel and Santa Barbara and Anacapa Islands. These areas belong to the Californian Biogeographic Province (Airamé *et al*., 2003b). Eastern Santa Rosa Island and Santa Cruz Island occupy a transition zone between the cold and warm water provinces, and should be considered a third biogeographic region (Seapy and Littler, 1980; Airamé *et al*., 2003b)

Within the Santa Barbara Channel, a localized cyclonic gyre circulation pattern exists year-round (Hendershott and Winant, 1996; Lagerloef and Bernstein, 1988) with seasonal variations in intensity. In general, cool water enters the channel from the west and flows eastward along the Channel Islands, while warm water enters the channel from the east and flows westward along the coast. Harms and Winant (1998) identify six distinct variations; *Upwelling, Relaxation, Cyclonic; Propagating Cyclones, Flood East, and Flood West*. In the *Upwelling* pattern, there is a strong south and southeastward flow of cool water from Point Conception and along the north sides of the Channel Islands, and a weak warm water flow toward the northwest along the mainland. In the *Relaxation* pattern, there is a strong northwestward flow of warm water into the channel from the east, and a weak inflow of cold water from the west. The *Cyclonic* pattern is an elongated, closed pattern created when the central eddy is strongest, and there is little flow into the channel from either the west or the east. In the *Propagating Cyclones* pattern, small, tight circular flow cells form in the center of the Channel and drift toward the west. These four patterns form in spring, summer and fall, but the cyclonicity is strongest in summer and weakest in winter. In the winter, directional flow patterns form. The winter *Flood East* pattern consists of a strong eastward flow into the Channel along the coastline, and lesser eastward inflow along the Channel Islands. The winter *Flood West* pattern has a strong northwestward flow along the coast, and a weaker northwest flow along the islands.

Two opposing forces generate the cyclonic flow patterns: a poleward pressure gradient and an equatorward wind stress (Nishimoto and Washburn, 2002). In the warm waters of the Southern California Bight, sea level is higher than in the cold, upwelled waters north of Point Conception. This difference in sea level creates a poleward pressure gradient that draws water westward through the channel. Upwelling-favorable winds tend to drive strong eastward flow, opposing the westward pressure gradient. When the effects of wind equal that of the pressure gradient, the cyclonic flow patterns form. Imbalances in the two competing forces create the pattern variations described above.

Nishimoto and Washburn (2002) found that the eddy circulation in the Santa Barbara Channel extended to depths of at least 650 feet (200 m), or nearly half the total channel depth, and suggest that persistent cyclonic eddies play an important role in maintaining marine populations through climate changes. Cold water uplifted in the center of the eddy may provide an additional source of nutrients during a shift to a warm-water regime, increasing primary productivity and the amount of food available for fish. Nishimoto and Washburn (2002) found large aggregations of juvenile fishes concentrated in an eddy in the Santa Barbara Channel, and suggest that high food availability and feeding success contributed to faster growth and higher survivorship of these fishes. Nishimoto and Washburn (2002) also noted that the fishes were entrained in the eddy current in their larval stages and remained there until they passed the juvenile stage, when they grew strong enough to escape the circulating current.

Hickey (2000) found that the sediments in ocean basins of the SCB are near anoxic to anoxic, and that the anoxic area is increasing. Expansion of the anoxic areas reduces the ability of the basin sediments to support marine life. The high ridges between the basins essentially prevent influx of oxygen-bearing water into the basins, which is important for maintaining oxygen levels. The events that bring oxygen to the basins are associated with processes in the upper water column. Strong upwelling and southeastward flow from the Santa Barbara Channel

into the Santa Monica Basin appear to drive cold, denser water over the ridges into the basins, where it mixes with the ambient water confined within. Influxes of oxygen-bearing cold water occur only for a few days at a time, after intervals of several years (Hickey, 2000). The Santa Barbara Basin, which lies between the Channel Islands and the mainland, is relatively shallow (1,640 ft/500 m). An intense coastal upwelling event off Point Conception caused rapid renewal of the water in this basin (Hickey, 1993). Within the last 40 years, water in the Santa Barbara Channel has overturned several times (Hickey, 1993).

Waves

Waves in the Santa Barbara Channel are produced by seasonal swells crossing the open ocean, the sheltering effect of Point Conception and the Channel Islands, the variable wind fields that arise from the mountainous coastal and island topography, and the complex shallow water bathymetry within the channel (O'Reilly *et al*., 2000). Deep water swells from winter storms typically enter the channel from the west or west-southwest, for the most part unbroken by the Channel Islands. West swells produce high waves along the south-facing coastline just south of Point Conception and at the eastern end of the channel south of Ventura. A massive fan of sediment deposited on the shelf by the Ventura and Santa Clara rivers concentrates much of the wave energy traveling eastward down the channel onto a narrow section of coastline near the mouth of the Santa Clara River channel (O'Reilly *et al*., 2000). When the deep water swell originates more from the west-southwest, this focusing zone shifts directly northward into the Ventura area. West swells can also produce large waves at Rincon Point west of Ventura, and at the south end of Santa Monica Bay near Redondo Beach. Wave heights increase along portions of the Channel Islands that border the south side of the channel (O'Reilly *et al*., 2000).

In the summer, deep water swells originate in the south Pacific, and encounter the Channel Islands as they move north toward California. The islands shelter most of the channel and the south-facing coast from summer swells, significantly limiting wave heights. South swells from storms near New Zealand enter the western end of the channel, while those originating further east near South America are almost entirely obstructed. South swells travel past Anacapa Island and reach the coast near Ventura and Rincon Point. Rare swells originating from the southeast can reach the coast at Santa Barbara (O'Reilly *et al*., 2000).

Long-Term Climate Perturbations

Longer term climatic phenomena influencing the region include El Niño, Pacific Decadal Oscillation, and global warming. The recurring El Niño-Southern Oscillation pattern is one of the strongest in the ocean-atmosphere system. El Niño is defined by relaxation of the trade winds in the central and western Pacific, which can set off a chain reaction of oceanographic changes in the eastern Pacific Ocean. Off the coast of California, El Niño events are characterized by increases in ocean temperature and sea level, enhanced onshore and northward flow, and reduced coastal upwelling of deep, cold, nutrient-rich water. During this period, survivorship and reproductive success of planktivorous invertebrates and fishes decrease with plankton abundance. Marine mammals and seabirds, which depend on these organisms for food, suffer food shortages, leading to widespread starvation and decreased reproductive success.

Every 20-30 years, the surface waters of the central and north Pacific Ocean (20°N and poleward) shift several degrees from the mean temperature. Such shifts in mean surface water temperature, known as the Pacific Decadal Oscillation, have been detected 5 times during the past century, with the most recent shift in 1998. The Pacific Decadal Oscillation impacts production in the eastern Pacific Ocean and, consequently, affects organism abundance and distribution throughout the food chain. Ocean waters off the coast of California have warmed considerably over the last 40 years. It is not clear if this warming is a consequence of an interdecadal climate shift or global warming. In response to these three phenomena, some species have shifted their geographic ranges northward, altering the composition of local assemblages.

2.4 PHYSIOGRAPHIC COMPLEXITY

Data and Methods

The rationale behind examining physiographic complexity is to provide potential linkages to spatial patterns described in other chapters, and to provide a measure of context for subsequent discussions of observed regional biogeographic patterns. For example, offshore circulation patterns in the region result, in part, from the interaction of large-scale ocean currents, local geography, and the unique basin and ridge topography of the ocean bottom of the Southern California Bight (Airamé *et al*., 2003a). As discussed in chapter 2.2, these currents influence the distribution of living marine resources in the region. Furthermore, many taxa, particularly fishes, are known

to exhibit a strong affinity for areas of high structural complexity (Yoklavich *et al*., 2000, 2002; Hixon *et al*., 1991; Hixon and Tissot, 1992; Field *et al*., 2002; Starr, 1998; and Williams and Ralston, 2002). The analyses presented here are provided as a proxy for quantifying structure in the region (i.e., mesoscale rugosity), and should be interpreted with care, as they represent an estimate for only one neighborhood range (1 km). Similar analyses can be performed for an infinite set of ranges, each resulting in similar patterns with dimensions proportionate to the prescribed neighborhood.

The maps of physiographic complexity presented here were derived using a bathymetric grid produced by the California Department of Fish and Game (CDFG) in August 2000 (Figure 2.1.1-Chapter 2.1.1). This bathymetric grid was made from 75 tiled digital elevation models (DEM) that were mosaicked into a single grid, and resampled to a 200 m resolution. DEM's were developed by the Teale Data Center under contract with CDFG, and have a geographic domain ranging from 31.9^{o} to 42.5^{o} north latitude. Physiographic complexity was calculated from these bathymetric data using a neighborhood statistical function in ArcView 3.2 (GIS), and represents the degree of variation in water depth (bathymetry) within a prescribed (and constant) area for the entire seascape. In this analysis, a standard deviation of water depth was calculated within a 1 km radius "moving-window". The calculated standard deviation was then assigned to the centroid of that neighborhood. This analysis was performed by centering the moving window on each individual bathymetric grid cell in the source data, and resulted in an estimate of the standard deviation of bathymetry at a scale of 1 km for the entire region (Figure 2.4.1, mapped range is 32° to 39°N). This measure of complexity was chosen over calculating a standard slope value because it not only captures areas of high slope, but also highlights areas that typify the unique basin and ridge topography of the ocean bottom in the Southern California Bight.

To analyze patterns of physiographic complexity in relation to proposed boundary concepts, average variance was calculated inside each of the boundaries. The assumption of this analysis was that encompassing an area of higher average complexity is preferred, and that this complexity likely provides a more diverse complement of potential habitats (niches) for living marine resources. Average complexity within each concept was then used in calculating an Optimal Area Index (OAI). Since the average is a relative measure of physiographic complexity, we also provide an analysis of the absolute area of high complexity captured within each concept. In this analysis, results of the complexity map were classified into standard deviations, with areas in red representing locations where the complexity was equal to or greater than 2 standard deviations above the mean deviation (henceforth "high"; stippled area in Figure 2.4.1). The total area of high complexity contained within each concept was then estimated for use in the absolute OAI calculations.

Broad-scale Patterns

The spatially-articulated estimate of physiographic complexity resulted in a map that highlights areas of steep slopes, as well as regions of ridge and basin topography. Stippled areas in Figure 2.4.1 indicate where average complexity was classified as high. A continuous northwest-southeast trending area of high complexity can be seen running along the entire coastline. This area represents the continental slope, and is generally centered on the 2,000 m isobath (shown in green). The large reticulated area of physiographic complexity that is evident throughout the Southern California Bight generally consists of the ridge and basin topography first described in chapter 2.1. In fact, nearly all of the high complexity areas contained within the current Channel Islands sanctuary boundary can be attributed to these unique geologic features of the continental borderland rather than to continental slope per se.

Results indicate that the complement of sanctuaries along the California coastline (Gulf of the Farallones, Cordell Bank, Monterey Bay, and Channel Islands) capture large areas of high estimated complexity, with each sanctuary comprised of at least 20% high complexity area. In this analysis (ranging from 31.9^{o} to 32.5^{o} north latitude), the total area identified as high complexity was 95,255 km^2. Roughly 8,251.1 km^2 (8.7%) of this area is contained within the four California sanctuaries, with 1.4% of the total falling inside the current boundaries of the Channel Islands National Marine Sanctuary. A total of 36% of the area contained within CINMS boundaries was classified as having high complexity. This is the second largest proportion of any California sanctuary (Gulf of the Farallones-21.5%, Cordell Bank-30.5%, and Monterey Bay-42%). Most of the complex area contained within the Gulf of the Farallones, Cordell Bank, and Monterey Bay national marine sanctuaries is comprised of continental slope. In the Monterey Bay sanctuary, much of the physiographic variance is attributed to the Monterey, Soquel, Carmel Canyon complex.

The continental slope drops steeply from the edge of the continental shelf (~200 m) to depths of approximately 3,000-4,000 m, where it reaches the abyssal plain. Waters of the continental slope are dark, cold, and under very high pressure. In general, the community structure of invertebrates and fishes along the continental slope vary markedly with depth (Airamé, *et al*., 2003a; NCCOS, 2003). This same trend is evident in the analysis of fish community structure presented in chapter 4.2, including those communities found in the ridge and basin structure of continental borderland in the Southern California Bight. Rockfishes (*Sebastes* spp.) and flatfishes (Pleuronectiformes) are some of the most common benthic fishes found inhabiting the region (Airamé, *et al*., 2003a). Because many ecologically and commercially important fishes and invertebrates exhibit a strong affinity for physiographic complexity (Gabriel and Tyler, 1980; Matthews and Richards, 1991; Sullivan, 1995; Williams and Ralston, 2002; Love *et al*., 2002; Field *et al*., 2002; NCCOS, 2003), and their community structure is often classified by ecologists based on the underlying metric (bathymetry), we consider higher complexity to be a benefit in this analysis. Overall, it is likely that concepts characterized by a wide range of depths, coupled with a high degree of complexity, would exhibit the greatest potential to support a diverse faunal assemblage. As such, optimal area index (OAI) values presented in here are designed to highlight concepts with the highest relative complexity.

Analysis of Boundary Concepts

Results of this analysis highlight expansive and interconnected areas of physiographic complexity throughout the Southern California Bight – an expression of the ridge and basin topography that dominates the regional geology. Nearly all of the high complexity areas contained within the current Channel Islands NMS boundary (No Action Concept; NAC) can be attributed to these unique features. A total of 24% of the area contained within current CINMS boundaries was classified as having high physiographic complexity. The optimal area index (OAI) values calculated for each concept suggest that only concept 5 provides greater benefit (in terms of physiographic variance), as it is the only boundary that resulted in a mean complexity value greater than the NAC.

As discussed in Chapter 1.4, two Optimal Area Index (OAI) values are presented here, the first of which is calculated using the mean complexity inside each of the concepts (henceforth “relative OAI”), and the second using the total area of high complexity captured inside each boundary (henceforth “absolute OAI”). Mean estimated complexity for the NAC was 21.2 with a coefficient of variation (CV) of 103.2%. Mean complexity and CV values for the remaining concepts, ranging from smallest in size to largest, are as follows: Concept 5-21.8, 100.2%; Concept 4-19.3, 110.6%; Concept 3-18.6, 113.7%; Concept 2-16.7, 111.4%; Concept 1a-18.5, 115.6%; and Concept 1-18.5, 115.6% (Figure 2.4.2). Mean complexity for the Study Area boundary (defined in McGinnis, 2000) was estimated to be 16.5 with a CV of 114.3% (Figure 2.4.2). The relatively large CV values resulted from the highly variable nature of the estimate (standard deviation of bathymetry). For example, areas along the continental shelf show relatively little deviation in bathymetry within a 1 km^2 neighborhood, while areas along the continental slope exhibit extreme differences in depth over short distances.

These results exhibit a weak, yet statistically significant (a=0.10) inverse relationship to concept size. This relationship is shown in Figure 2.4.3 as a linear regression function between concept area (km^2) and the mean complexity value calculated within the boundary (r^2=0.43, P=0.08). On the other hand, the relationship between concept area and absolute area of high complexity was very predictable (and statistically significant), with larger concepts containing ever larger areas of high complexity. Figure 2.4.3 shows the linear regression function between the total concept area (km^2) and the area of high complexity contained within the boundary (r^2=0.98, P<0.0001).

A more balanced metric to use in assessing the relative benefits of each concept as it relates to optimizing for high physiographic complexity is the OAI (Table 2.4.1, also see Chapter 1.4). While this metric decouples the relationships between concept area and the relative and/or absolute estimate to some extent, results of the OAI are still dependent upon the input data, absolute vs. relative measures. As such, we’ve provided OAI results for both mean and total area of high complexity. Results suggest that Concept 5, the minimum expansion concept, provides maximum benefit in terms of the mean complexity calculated for each concept (relative OAI) and in terms of the area of high complexity contained within each concept (absolute OAI). Because the mean OAI incorporated a negative value in the numerator for all boundary concepts except 5 (decreased complexity), the calculated value is necessarily negative.

Summary

• Patterns of mean physiographic complexity highlight areas along the continental slope, as well as areas typical of ridge and basin topography.

• Scientific literature supports the notion that many biological communities exhibit affinities for high complexity, and are often classified based on the underlying bathymetry estimate.

• Of the boundary concepts under consideration, Concept 5 provides relatively large increases in relative and absolute physiographic complexity for its size.

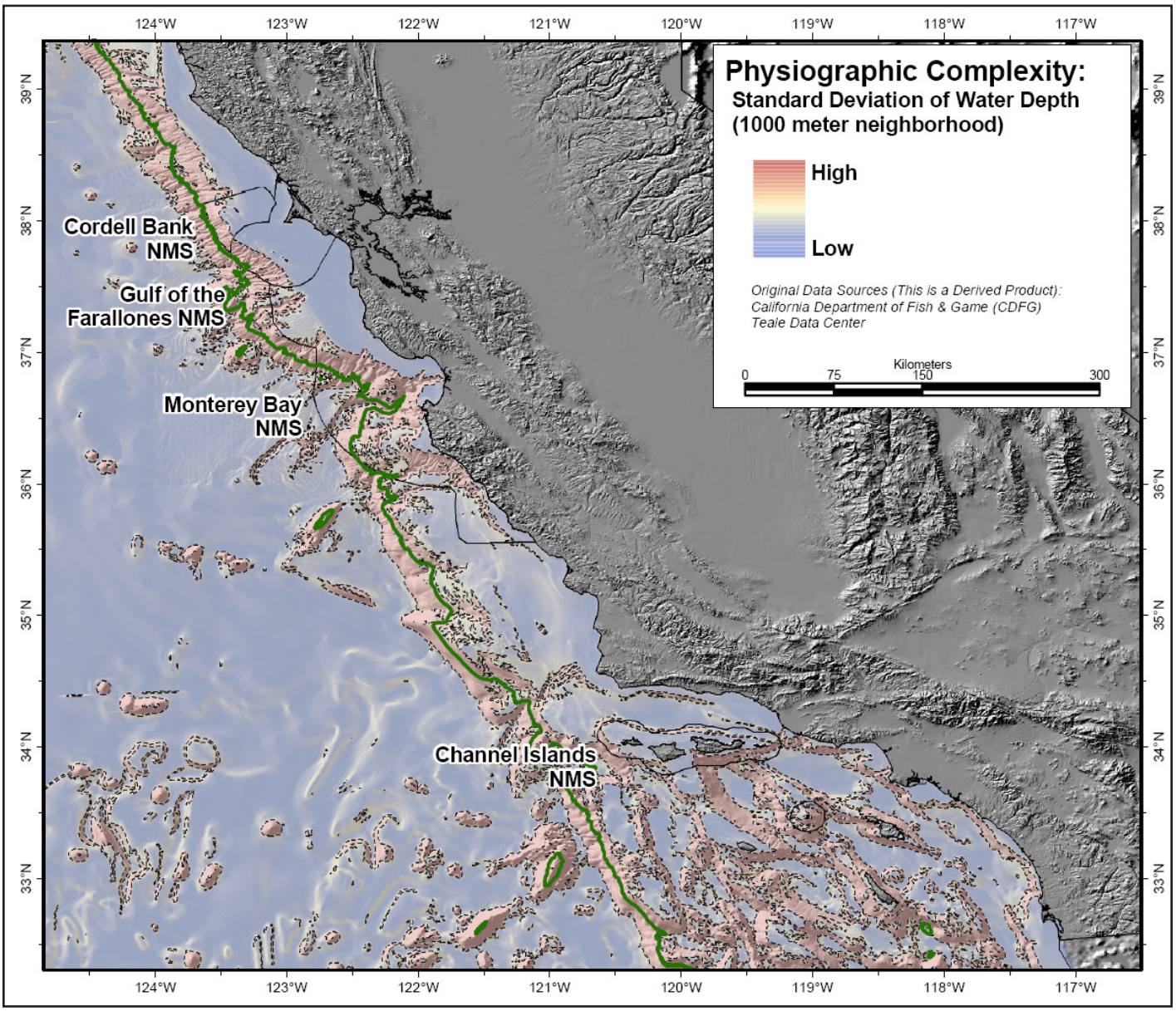

Figure 2.4.1. Map of physiographic complexity along the California coast (ranging from 32° to 39°N). Stippled areas indicate where complexity was >2 standard deviations above the mean. The green line demarcates to 2000 m isobath (a proxy for the continental slope).

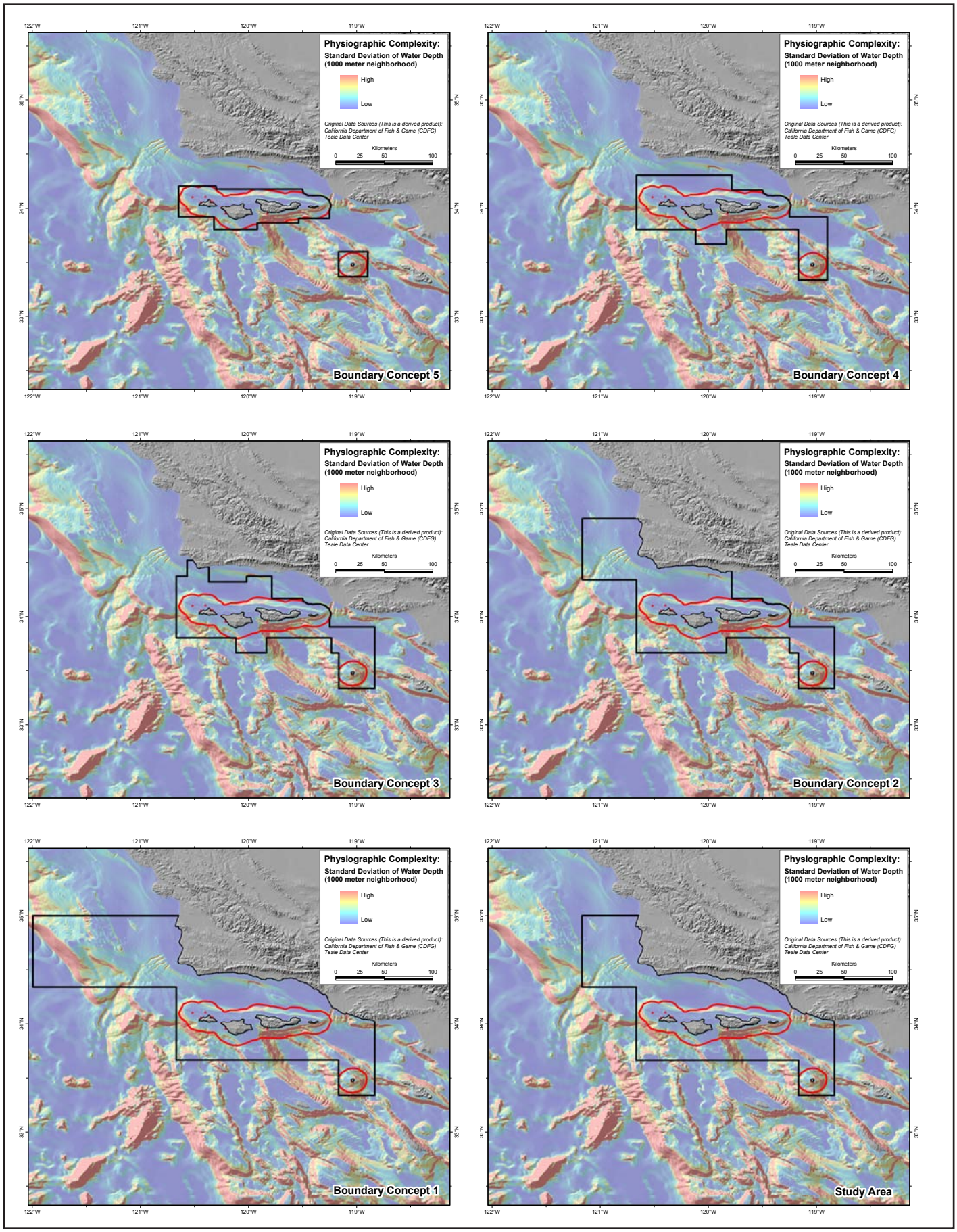

Figure 2.4.2. Physiographic complexity within boundary concepts. The No Action Concept (NAC) is shown as a red line, while the concepts are shown as a black line.

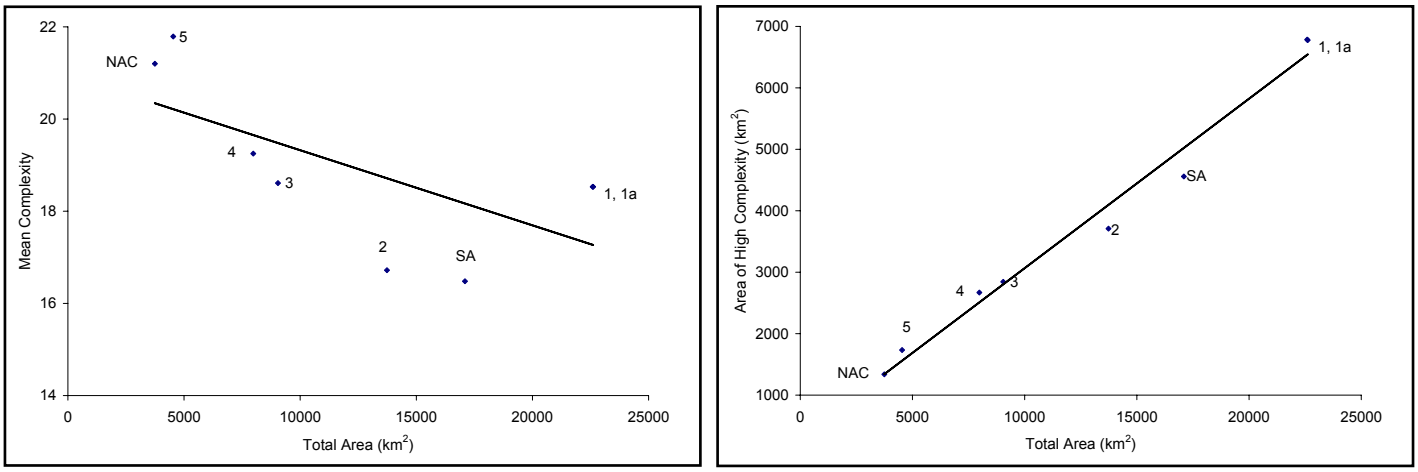

Figure 2.4.3. Linear regression functions between concept area (km^2) and mean physiographic complexity (left), and the area (km^2) of high physiographic complexity (right).

Table 2.4.1. Analysis of boundary concepts. Numbers in bold indicate an increase in the estimate when compared to the No Action Concept (NAC). Maximum calculated OAI numbers are shaded in gray. Delta (Δ) indicates a rate of change calculation, and is always expressed as a percent change from the NAC.

Concept	Area (km^2)	Mean Complexity	High Complexity Area (km^2)	Δ Area (%)	Δ Mean Complexity (%)	Δ High Complexity Area (%)	Mean Complexity OAI (relative)	High Complexity Area OAI (absolute)
NAC	3745	21.20	1339	-	-	-	-	-
5	4536	**21.79**	**1734**	21.12	2.78	29.51	0.132	1.397
4	7981	19.25	**2669**	113.11	-9.20	99.31	-0.081	0.878
3	9044	18.61	**2844**	141.50	-12.22	112.37	-0.086	0.794
2	13736	16.72	**3709**	266.78	-21.13	177.00	-0.079	0.663
1a	22591	18.53	**6777**	503.23	-12.59	406.15	-0.025	0.807
1	22613	18.53	**6785**	503.82	-12.59	406.76	-0.025	0.807
SA	*17093*	*16.48*	**4558**	*356.42*	*-22.26*	*240.39*	*-0.062*	*0.674*

2.5 BENTHIC SUBSTRATE

Data and Methods

In this chapter, geologic data for offshore California are analyzed to characterize the distribution of substrate types, and more specifically for the area around the Channel Islands National Marine Sanctuary. Analyses are based upon a comprehensive set of geologic data that were synthesized, classified, and mapped according to substrate and habitat type for the entire U.S. west coast. Benthic features from a variety of sources (side-scan sonar, bottom samples, seismic data, and multibeam bathymetry) were interpreted by geologic mapping experts and subsequently classified according to substrate and habitat type (Greene *et al.*, 1999). This task was completed by the National Marine Fisheries Service (NMFS) as part of the development of an Environmental Impact Statement (EIS) that considers the designation of Essential Fish Habitat (EFH) for Pacific coast groundfish (NMFS, 2004).

The substrate data ranges from Washington to the U.S.-Mexico border (32°-48.5° latitude) and from 50-200 km from the shoreline (excluding estuaries). Benthic substrate data for California encompasses nearly 165,000 km^2 of the continental shelf and slope and are classified into approximately 33 different habitat types (Figure 2.5.1). The level of spatial resolution varies across the dataset based on the quantity and quality of the original data sources used to construct this substrate map. As such, fine scale inaccuracies may exist throughout the range of the data.

In addition to assessing the distribution of substrate types throughout the southern California region, the map was used as an input for deterministic habitat suitability models (HSM) for a select group of fishes and inverte-

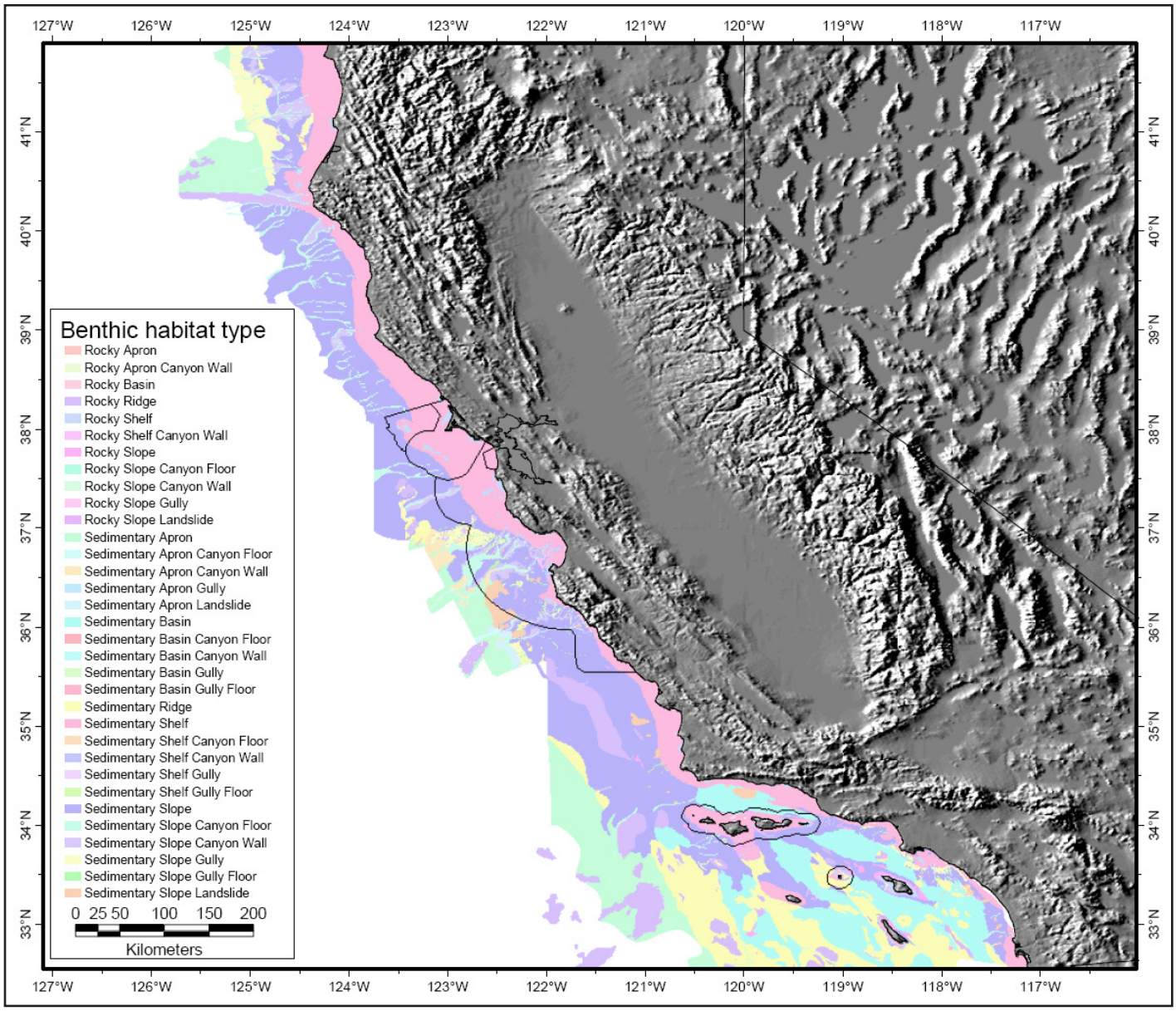

Figure 2.5.1. Benthic habitat types for the marine waters off California (Greene *et al*., 1999).

brates (Chapters 3.1 and 4.1). Linking the 33 classes of habitat types to species life history information from scientific literature was difficult; thus, a separate substrate attribute was used for habitat suitability modeling which defined the substrate as either hard or soft. Model results for invertebrates were reviewed in June 2004 by a panel of experts. They expressed concern that the map underestimated the amount of hard bottom, most notably at depths between 0-30 m along the mainland south of Point Conception and around the Channel Islands. Additional hard substrate data (MMS, 1987) were then provided by scientists from UCSB who converted non-digital substrate maps developed by the Minerals Management Service (MMS) into a format suitable for use within a GIS. These data extend from Morro Bay to the U.S.-Mexico border and were combined with the NMFS substrate data, resulting in a better estimation of hard substrate in southern California (Figure 2.5.2). Chapter 2.6 provides a more detailed analysis of these data.

Broad-scale Patterns

Figure 2.5.3 displays the distribution of 33 habitat types off the coast of California encompassing a total area of 164,725 km^2. Habitat types shaded in red reflect rocky outcroppings, ridges, reefs, and other hard bottom features. Areas shaded with orange and yellow generally display soft continental shelf substrate, while areas in green indicate soft substrate on the continental slope. The amount of area classified as hard bottom habitat accounts for approximately 10% of the total area, the majority of which is located south of Monterey Bay. The region

Table 2.5.1. Area (km^2) and percentage of total area for habitat types within boundary concepts.

Habitat Type	NAC		Concept 5		Concept 4		Concept 3		Concept 2		Concept 1a		Concept 1		Study Area	
	Area	%	Area	%	Area	%	Area	%	Area	%	Area	%	Area	%	Area	%
Rocky Ridge (hard)	33.9	0.9	44.6	1.0	106.7	1.4	125.0	1.4	158.9	1.2	880.4	3.9	884.3	3.9	201.4	1.2
Rocky Shelf (hard)	135.8	3.6	137.6	3.0	163.5	2.1	187.9	2.1	236.6	1.7	264.9	1.2	263.2	1.2	265.0	1.6
Rocky Slope (hard)	120.6	3.2	157.8	3.5	265.1	3.3	284.5	3.3	325.2	2.4	366.5	1.6	365.4	1.6	366.7	2.1
Rocky Slope Canyon Wall (hard)	0	0	0.1	<0.01	0	0	0	0	0	0	0	0	0	0	0	0
Sedimentary Apron (soft)	0	0	0	0	0	0	0	0	0	0	1338.5	5.9	1333.8	5.9	0	0
Sedimentary Basin (soft)	379.8	10.2	640.6	14.2	2371.8	29.8	2772.8	30.7	3026.6	22.1	3812.2	16.9	3806.1	16.9	3817.1	22.4
Sedimentary Ridge (soft)	235.5	6.3	302.1	6.7	342.9	4.3	347.7	3.8	409.3	3.0	968.9	4.3	965.6	4.3	460.2	2.7
Sedimentary Shelf (soft)	1877.9	50.4	1934.0	42.8	2162.1	27.1	2360.3	26.1	3681.6	26.8	5026.6	22.3	5038.2	22.4	5049.2	29.6
Sedimentary Shelf Canyon Wall (soft)	5.7	0.2	5.7	0.1	5.7	0.1	5.7	0.1	5.7	<0.01	5.7	<0.01	5.7	<0.01	5.7	<0.01
Sedimentary Shelf Gully Floor (soft)	0.7	<0.01	0.7	<0.01	0.7	<0.01	0.7	<0.01	0.7	<0.01	0.7	<0.01	0.7	<0.01	0.7	<0.01
Sedimentary Slope (soft)	832.8	22.4	1167.7	25.8	2313.9	29.0	2596.0	28.8	5330.4	38.8	9222.6	41.0	9214.2	40.9	5309.3	36.9
Sedimentary Slope Canyon Floor (soft)	21.3	0.6	32.3	0.7	88.7	1.1	88.4	1.0	137.1	1.0	137.6	0.6	137.6	0.6	137.8	0.6
Sedimentary Slope Canyon Wall (soft)	81.6	2.2	99.0	2.2	98.8	1.2	110.9	1.2	111.0	0.8	186.9	0.8	186.9	0.8	157.6	0.9
Sedimentary Slope Gully Floor (soft)	0	0	0	0	0	0	0	0	21.2	0.2	18.6	0.1	21.2	0.1	21.2	0.1
Sedimentary Slope Landslide (soft)	0	0	0	0	46.3	0.6	148.8	1.6	277.3	2.0	284.5	1.3	284.3	1.3	284.5	1.7
∑ hard	290.2	7.8	340.2	7.5	537.2	6.7	597.3	6.6	720.8	5.3	1511.8	6.7	1512.8	6.7	833.0	4.9
∑ soft	3435	92.2	4182	92.5	7431	93.3	8433	93.4	13001	94.7	21003	93.3	20994	93.3	16243	95.1

north of Monterey is typically characterized by a broad continental shelf and slope comprised of soft substrate with scattered areas of hard bottom. In southern California, the area appears to be dominated more by sedimentary basins, ridges, and slope habitat. Large features are noticeable throughout the extent of the data: the Gorda Escarpment due west of Cape Mendocino, Cordell Bank west of Point Reyes, and the Davidson Seamount and Santa Lucia Bank southwest of Monterey Bay. In southern California, hard bottom areas are observed comprising features such as the Rodriguez Seamount, San Juan Seamount, Patton Escarpment, Cortes Bank, and Tanner Bank. Soft bottom features that are readily apparent are the basins of Monterey Canyon, Pioneer Canyon, and the Santa Barbara-Ventura Canyon in southern California.

Analysis of Boundary Concepts

Figure 2.5.3 displays benthic habitat types in southern California. Fifteen of the 33 habitat types found across California are found within the study area (Table 2.5.1). Percentages of hard substrates ranged from 5-8% of the total area within concept boundaries. Most hard substrate was located south of San Miguel and Santa Rosa Islands, around Anacapa Island and north of Santa Barbara Island. Concept 1a contained the most hard substrate (1,514 km^2), mostly attributed to the inclusion of the southern portion of Santa Lucia Bank. Soft substrates were mostly comprised of sedimentary shelf, slope, and basin habitat classifications (Table 2.5.1).

Spatial heterogeneity of habitats was quantified using the Shannon Index of diversity, and was compared among boundary concepts. This approach has been recently applied to marine coral reef ecosystems (Jeffrey, 2005). The Shannon index (Shannon and Weaver, 1949) is one of the most commonly used diversity metrics in community ecology (Magurran, 1988). Typically, the index is used to characterize biological communities; however, the same principles apply when analyzing the habitat map. The index attempts to balance habitat richness (the number of unique habitat types) with habitat evenness (the amount of area among the habitat types). For a given number of habitat types, the Shannon index is highest when there are equal areas within each habitat type. The Shannon index (H') was calculated using the formula:

$$H' = -\sum_{i=1}^{S} \left[\left(\frac{n_i}{N} \right) \ln \left(\frac{n_i}{N} \right) \right]$$

where n_i is the total area of the ith habitat type (S) in the sample, and N is the total area of the sample (Magurran, 1988).

We supplement Shannon's Index of diversity with a measurement of evenness calculated using Shannon's equitability index:

$$E = H' / \ln (N)$$

Values of this index range from 0 to 1 and describe the dominance of habitat types; values close to 1 indicate that habitats are evenly distributed.

Figure 2.5.4 shows the calculated habitat diversity for each of the boundary concepts and the Study Area. Habitat diversity was lowest within the current boundary and increased with increasing concept area, with the exception of Concept 2, which had the third lowest diversity. Similarly, habitat richness (the total number of habitat types present) was lowest within the current boundary and increased with increasing concept area (Figure 2.5.5). Concept 2 and the study area exhibited low evenness values and displayed similar trends to diversity values. As expected, habitat richness increased as concept area increased, as well as diversity for 4 of the 6 concepts. Diversity and evenness values for the Study Area and Concept 2 were the lowest (Figure 2.5.5). While the area of new habitats gained for Concept 2 and the study area were large, these gains were dominated by two habitat types. Thus habitat diversity and evenness values were depressed.

Although habitat diversity was greatest within Concept 1a (Figure 2.5.6) and was not statistically significant (r^2=0.44, p<0.17), analysis of diversity using the OAI (Table 2.5.2) indicate that Concept 5, the minimum expansion concept, provides the greatest benefit in terms of the proportional changes in area and diversity.

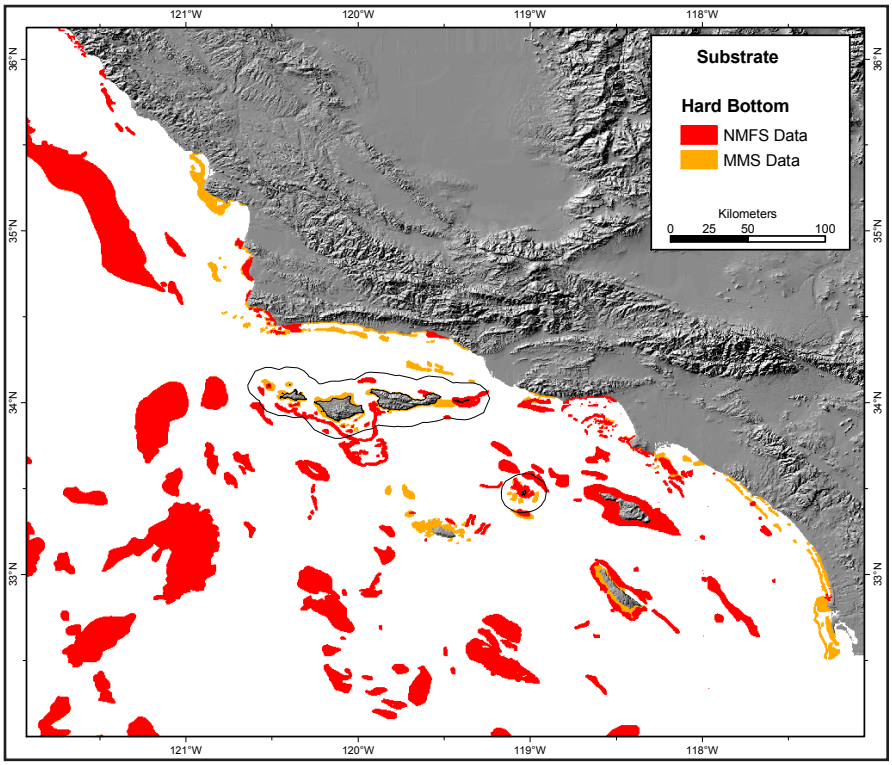

Figure 2.5.2. Location of hard substrate from NMFS and MMS datasets.

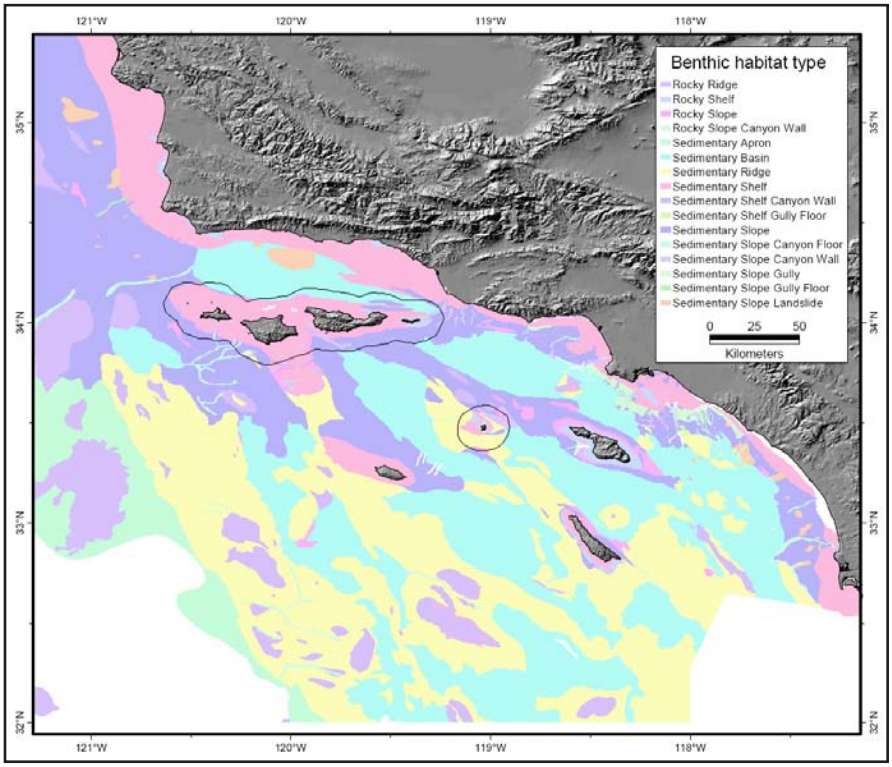

Figure 2.5.3. Benthic habitat types for the marine waters off southern California (Greene *et al.*, 1999).

Summary

• Data presented here provide the most current broad-scale representation of benthic habitats for the contiguous coastline of the western U.S.

• Patterns of habitat diversity and richness were positively correlated with the increasing area of boundary concepts.

• Of the six boundary concepts being considered, Concepts 1 and 1a provided the highest habitat diversity and richness, but Concept 5 ranked highest in the OAI.

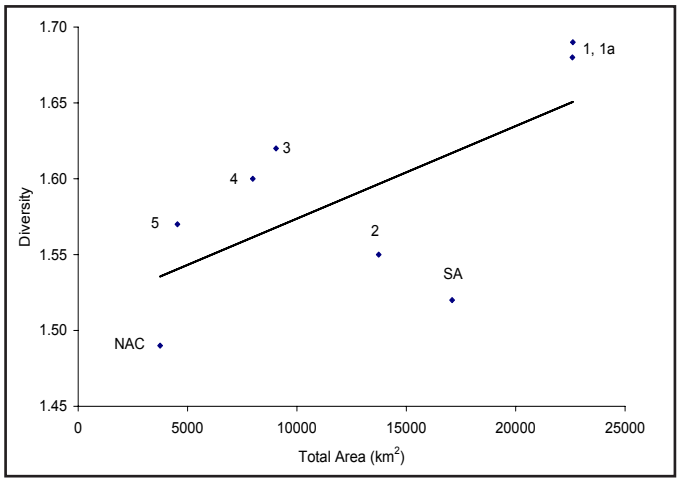

Figure 2.5.4. Regression of habitat diversity and total area for the current and proposed boundary concepts. Numbers indicate concepts and NAC=No Action Concept, SA=Study Area.

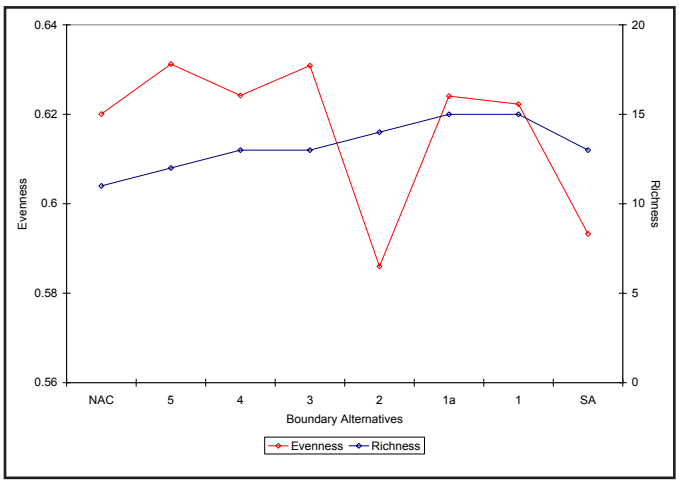

Figure 2.5.5. Evenness and richness estimates for habitat types within boundary concepts. Numbers on the x-axis represent concepts, NAC=No Action Concept, SA=Study Area.

Table 2.5.2. Analysis of habitat diversity within boundary concepts. Numbers in bold indicate an increase in the estimate when compared to the No Action Concept (NAC). Maximum calculated OAI numbers are shaded in gray. Delta (Δ) indicates a rate of change calculation, and is always expressed as a percent change from the NAC.

Concept	Area (km²)	Diversity (H´)	Δ Area (%)	Δ Diversity (%)	OAI (absolute)
NAC	3475	1.49	-	-	-
5	4538	**1.57**	21.12	5.37	0.25
4	7981	**1.60**	113.11	7.38	0.07
3	9044	**1.62**	141.50	8.72	0.06
2	13736	**1.55**	266.78	4.03	0.02
1a	22591	**1.69**	503.23	13.42	0.03
1	22613	**1.68**	503.82	12.75	0.03
SA	*17093*	*1.52*	*356.42*	*2.01*	*0.01*

2.6 BATHYMETRIC LIFE-ZONES

Data and Methods

This section describes the geographic distribution of habitats of southern California classified by substrate type and depth. Within the region, bathymetry ranges from intertidal to over 4,000 m, and four zones have been recognized within this range which contain distinct biological communities (Airamè *et al*., 2003b). Within the top 30 m, light penetrates surface waters, supporting a highly productive nearshore community. Shallow rocky reefs often support kelp forests that provide physical structure and an abundant source of food for subtidal organisms. Soft bottom habitats lack the physical structure and high production associated with kelp forests and rocky reefs and are commonly inhabited by many species of groundfish and invertebrates (Airamé *et al*., 2003a). Many species of rockfish and rock crabs inhabit rocky reefs at depths between 30-100 m, while several species of flatfish and molluscs occupy soft substrates. At depths of 100-200 m, rockfish such as bocaccio and cowcod, are common on rocky reefs, while several species of prawns inhabit soft substrates. Continental slope species such as sablefish, thornyheads, and dover sole inhabit hard and soft substrates at depths >200 m.

The previous section assessed the distribution of substrate types in the vicinity of the Channel Islands National Marine Sanctuary (CINMS). In this section, benthic substrate from the combined NMFS and MMS datasets is used in conjunction with bathymetry contours to provide a two-dimensional assessment of habitats within each boundary concept. Bathymetry is also categorized into four depth categories, according to the classifications described in Airamé *et al*., (2003b):

0-30 m	Shoreline, photic zone
30-100 m	Upper continental shelf
100-200 m	Lower continental shelf
>200 m	Continental slope

Habitat diversity is a measure of both richness (the total number of habitat categories present) and the evenness of their distribution. All eight of the combinations of bathymetry categories (0-30 m, 30-100m, 100-200m, >200m) and substrate groups (hard, soft) are present in the current CINMS boundaries (Airamé *et al*. 2003b), and thus in all of the boundary concepts. Therefore, richness is equivalent in all of the boundary concepts, and we can reduce our analysis to a discussion of the spatial evenness of the eight habitat combinations. Shannon's equitability (E_H) is a common metric used to describe evenness and can be calculated using the formula:

$$\frac{-\sum_{i=1}^{S}\left[\left(\frac{n_i}{N}\right)\ln\left(\frac{n_i}{N}\right)\right]}{\ln(S)}$$

where n_i is the area of habitat belonging to the ith habitat type (S) in the boundary concept, and N is the total area of the boundary concept. Thus, n_i/N is the proportion of habitat type i relative to the total area of that boundary concept (Magurran, 1988). Values for Shannon's Equitability range from 0 to 1 with 1 being complete evenness.

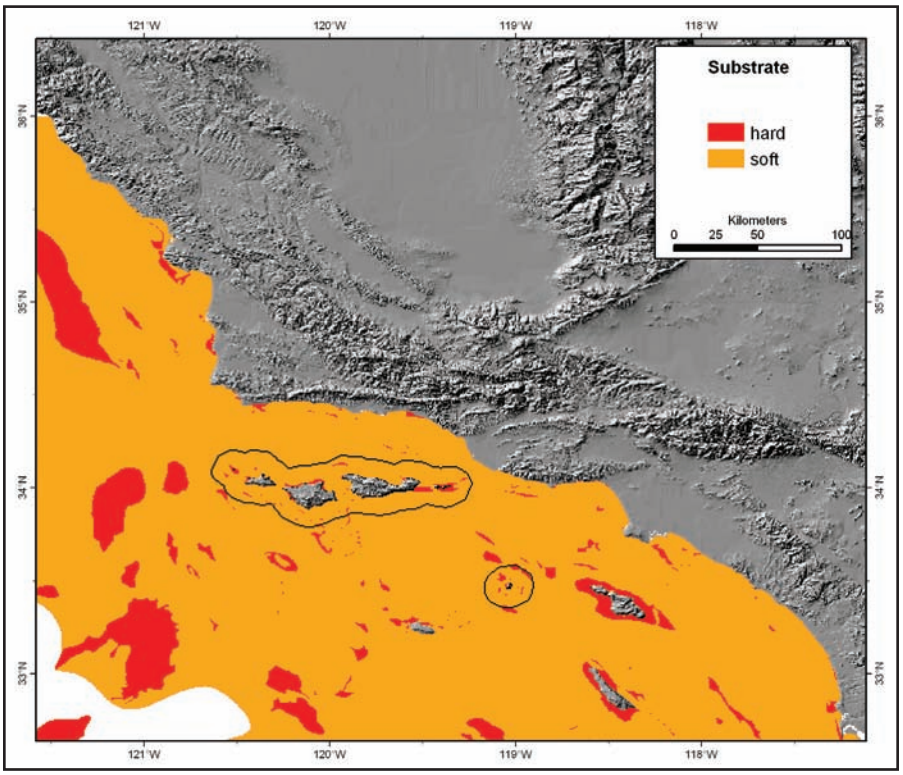

Figure 2.6.1. Distribution of benthic substrate types (hard or soft) off southern California.

Broad-scale Patterns

Rocky habitats are patchy both along the coastline as well as further offshore (Figure 2.6.1); however, much of the nearshore habitat around the Channel Islands is comprised of hard substrate. Depths greater than 200 m are a dominant feature of the broad-scale bathymetry (Figure 2.6.2). Habitats within the upper continental shelf (30-100 m) are

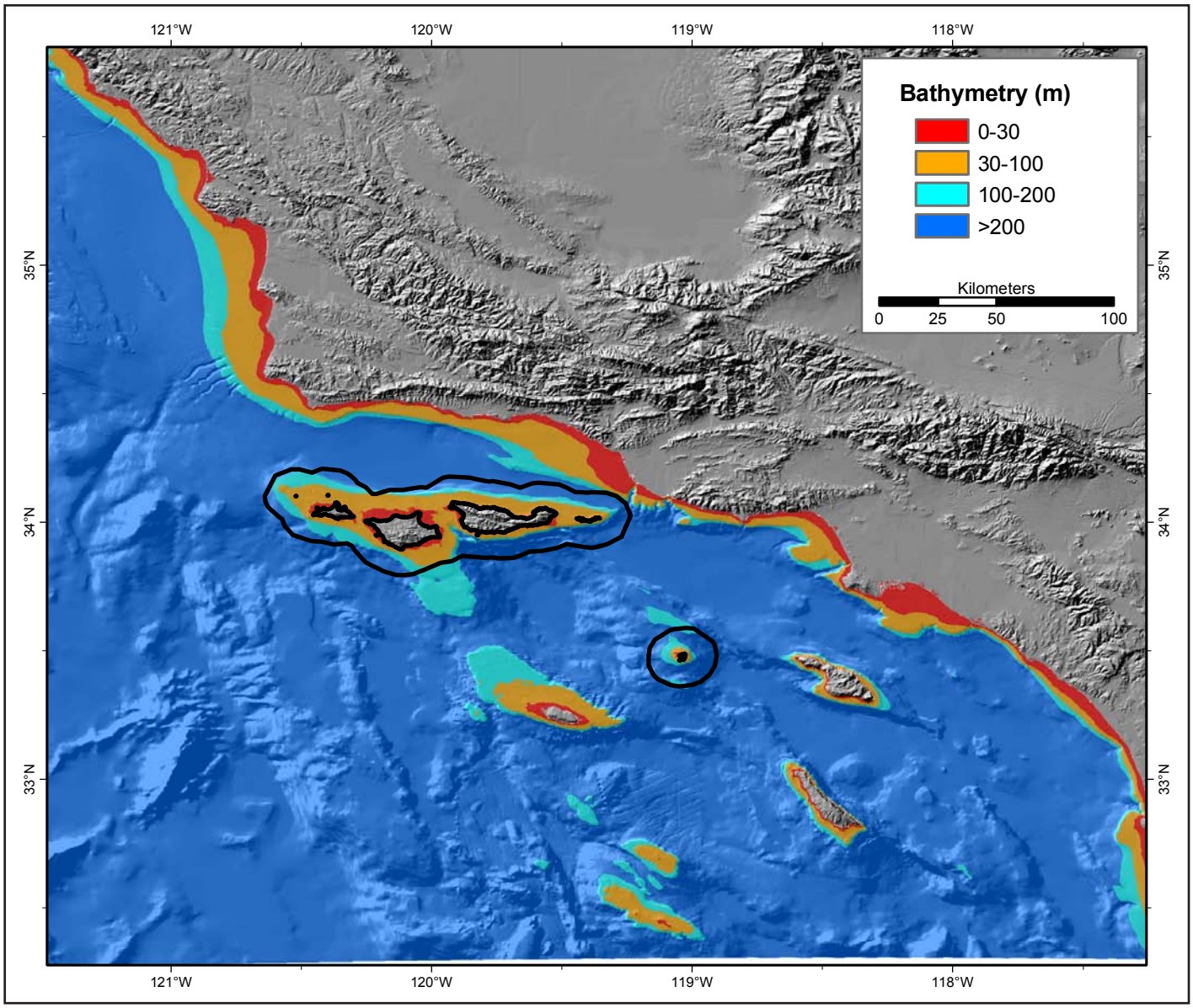

Figure 2.6.2. Distribution of bathymetric zones (m) off southern California.

the second most common, followed by lower continental shelf habitat (100-200 m). Shoreline habitats within the photic zone (0-30 m) are the least abundant.

Analysis of Boundary Concepts

All configurations considered here were dominated by soft substrate, which covered more than 85% of the total area within each concept (Figure 2.6.1). Likewise, depths greater than 200 m were predominant and increased as concept area increased (Figure 2.6.2). These continental slope habitats comprise 43% of the area within the current boundary, 67% of the Study Area, 51% of Concept 5, 68% of Concept 4, 69% of Concept 3, 70% of Concept 2, and 75% of Concepts 1 and 1a. Upper continental shelf followed in habitat dominance ranging from 31% for the current boundary to 12 for Concepts 1 and 1a. Relative abundance also declined with increasing concept area.

Evenness of the eight habitat categories generally declined as area increased, and was greatest for the No Action Concept (Table 2.6.1). This trend is graphically represented in Figure 2.6.3 as a linear regression function between area (km^2) and evenness (r^2=0.66, p=0.01). This trend can primarily be attributed to the disproportionate gain in deeper habitat as more area is incorporated into a boundary concept. The current CINMS boundaries and the smaller concepts 5 and 4 are a more suitable choice based upon evenness alone.

A more balanced metric to use in assessing the relative representation of habitat types and depth is the Optimal Area Index (OAI) (Table 2.6.1). OAI takes into account the proportional change (%) in evenness moving from the NAC to each of the concepts under consideration. It also incorporates the proportional change (%) in area from the NAC. The negative value of the OAI for habitat evenness for all of the boundary concepts under consideration indicates that the current CINMS boundary is preferable. Compared to the other concepts, the NAC contains a more equitable distribution of the 8 habitat categories.

Table 2.6.1. Analysis of life-zone evenness within boundary concepts. Numbers in bold indicate an increase in the estimate when compared to the No Action Concept (NAC). OAI estimates shaded in gray represent maximum observed benefit. Delta (Δ) indicates a rate of change calculation, and is always expressed as a percent change from the NAC.

Concept	Area (km^2)	Evenness	Δ Area (%)	Δ Evenness (%)	OAI (absolute)
NAC	3475	0.78	-	-	-
5	4538	0.73	21.12	-5.69	-0.27
4	7981	0.59	113.11	-23.87	-0.21
3	9044	0.58	141.50	-25.60	-0.18
2	13736	0.56	266.78	-27.80	-0.10
1a	22591	0.53	503.23	-31.27	-0.06
1	22613	0.53	503.82	-31.25	-0.06
SA	17093	0.59	356.42	-24.32	-0.07

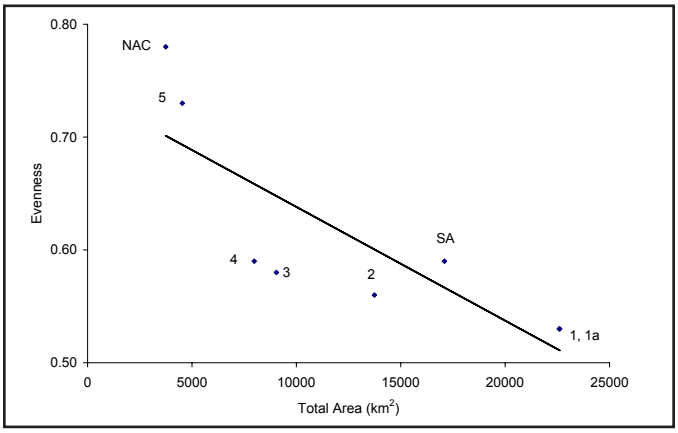

Figure 2.6.3. Regression of habitat evenness and total area for the current and proposed boundary concepts. Numbers indicate concepts and NAC=No Action Concept, SA=Study Area.

Summary

• Upholding ecosystem biodiversity requires protection of a wide variety of representative and unique habitats. Habitat in Central and Southern California can be characterized by a range of substrate types and depths that provide structure for a variety of organisms, including kelp forest, soft bottom and rocky reef communities.

• Similar to the broad-scale patterns, the current boundary of the CINMS encompasses a considerable amount of soft substrate. The bathymetric classes considered here (photic zone, upper and lower continental shelf, and continental slope) are all represented within the region and within the current CINMS boundaries where they are distributed with a relatively high degree of evenness.

• The current CINMS boundary provides a more equal representation of habitats (substrate type and depth) than the proposed boundary concepts.

2.7 SEA SURFACE TEMPERATURE AND FRONTAL BOUNDARIES

Pattens in sea surface temperature (SST) influence the distribution of marine species and habitats, particularly in areas of persistent SST fronts. The convergence of the northern and southern biogeographical provinces near the Santa Barbara Channel result in a dynamic biological and physical transition zone which influences the abundance and distribution of many organisms, including pelagic juvenile fishes, plankton and other microorganisms, benthic macroalgae, seagrasses, and invertebrates. Large-scale shifts in SST, and consequently frontal boundaries, affect the spatial and temporal distribution of these organisms. This chapter provides analysis of SST and frontal boundaries for the region of interest and provides physical context for subsequent biological analyses.

Data and Methods

The sea surface temperature (SST) data presented here were obtained from the NOAA/NASA Pathfinder dataset. SST data are derived from the 5-channel Advanced Very High Resolution Radiometers (AVHRR); multi-purpose imaging instruments attached to the NOAA -7, -9, -11 and -14 polar orbiting satellites. They measure global cloud cover, sea surface temperature, and ice, snow and vegetation cover and characteristics. Daily, 8-day, and monthly averaged data for both the ascending pass (daytime) and descending pass (nighttime) are available on equal-angle grids of 4096 pixels/360 degrees (nominally referred to as the 9 km resolution), 2048 pixels/360 degrees (nominally referred to as the 18 km resolution), and 720 pixels/360 degrees (nominally referred to as

the 54 km resolution or 0.5 degree resolution). Monthly averaged 9km data were used here to achieve the greatest possible spatial resolution and to minimize cloudiness (no data values) by averaging cloud-free data values across a month of data. The SST data encompassed 125 months from January 1993-May 2003. The AVHRR Oceans Pathfinder SST data were obtained through the online PO.DAAC Ocean ESIP Tool (POET) at the Physical Oceanography Distributed Active Archive Center (PO.DAAC), NASA Jet Propulsion Laboratory, Pasadena, CA. <http://podaac.jpl.nasa.gov/poet>.

To analyze spatial patterns in relation to proposed boundary concepts, sea surface temperature data for the 125 months (January 1993-May 2003) were averaged across four months (January, April, July, October) representing typical seasonal temperature values, to provide an overall estimate of mean SST along the Pacific margin of the coterminous United States (ranging from 31°-46°N, Figure 2.7.1). Average SST was calculated for each of the months across all years for which data were available. In addition to sea surface temperature, we also present estimated SST variance over time and an analysis of frontal boundaries and their persistence through time as derived from SST data. Variance in SST over time was estimated for each cell by calculating the statistical variance of all data available in that cell from January 1993-May 2003 (Figure 2.7.2). Variance estimates ranged from 0 to 10.6. The resulting map was classified into four equal area quantiles. Two quantiles representing the areas of least variance were highlighted (0-25% and 25-50%).

Frontal boundaries were derived from SST data using a number of tools that make up the Generic Mapping Tool (GMT) software package developed and maintained by Paul Wessel (University of Hawaii) and Walter H. F. Smith (NOAA). GMT is available under the GNU public license and can be downloaded from the University of Hawaii, Honolulu, HI <http://gmt.soest.hawaii.edu>. To derive frontal boundaries, each monthly mean SST dataset was first converted to GMT's grid format using the GMT tool *nearneighbor* (Figure 2.7.3). A slope function was run across each of these monthly SST coverages using GMT *grdgradient* to create new coverages in which the magnitude of the slope was calculated for each cell. In this case, the slope represents areas containing the steepest temperature gradient, or changes in SST, across some geographic extent space. The resulting coverage was then classified into 20 equal areas (5% quantiles) using GMT *grdhisteq* and the quantile with the greatest slope was extracted using GMT *grdclip* to represent the areas with the steepest temperature gradients (Figure 2.7.3). These areas of steep temperature gradient serve as a proxy for SST fronts. The resulting grids were added together using GMT *grdmath* to obtain a final grid containing cells with values representing the number of months during which an SST front occurred in each cell (Figure 2.7.4). This coverage of SST frontal persistence contained cell values ranging from zero to 65 months and was classified into standard deviations. The highest standard deviation (+3 above the mean, or 21-66 of the 125 available months) was considered to represent areas of persistent SST fronts.

Broad-scale Patterns

Broad-scale patterns referred to in this section include consideration of both spatial and temporal scales. It is understood that sea surface temperature patterns and their related features are ephemeral depending on the season, year, and the state of the El Niño-Southern Oscillation (ENSO). However, because sanctuary boundaries do not change seasonally, or with the ENSO, a decision was made to look at the overall spatial and temporal trends through both space and time to evaluate the mean expression of SST and its effects.

Sea surface temperature analysis displays the expected gradient of cold water in the north slowly warming towards the south, ranging from 0° to 23° Celsius. Of particular interest is that seasonal changes that bring warmer water to the north coincide with the onset of coastal upwelling along the northern California coast (Figure 2.7.1). The end result is that water temperatures along the northern California coast remain cool during the summer months and are at times cooler in the summer than during winter months. The expression of this system is most evident in the low variance in SST exhibited along the coast from the northern California border to Point Conception (Figure 2.7.2). This core of cool water provides a relatively stable environment that may contribute to apparent formation of northern and southern biogeographic provinces, and the formation of a transitional zone between them that is often ascribed to the Channel Islands area (McGinnis, 2000).

Analysis of potential SST frontal zones (Figures 2.7.4 and 2.7.5) suggest that the Channel Islands region exhibits a persistent concentration of steep temperature gradients. Persistent concentrations of high frontal density are not present all the time. These frontal systems are defined not as a single persistent front, but as a dynamic region characterized by a persistent high concentration of frontal features. In the analysis (ranging from 31°-47° degrees latitude), the total area defined as having a high concentration of persistent SST fronts was roughly

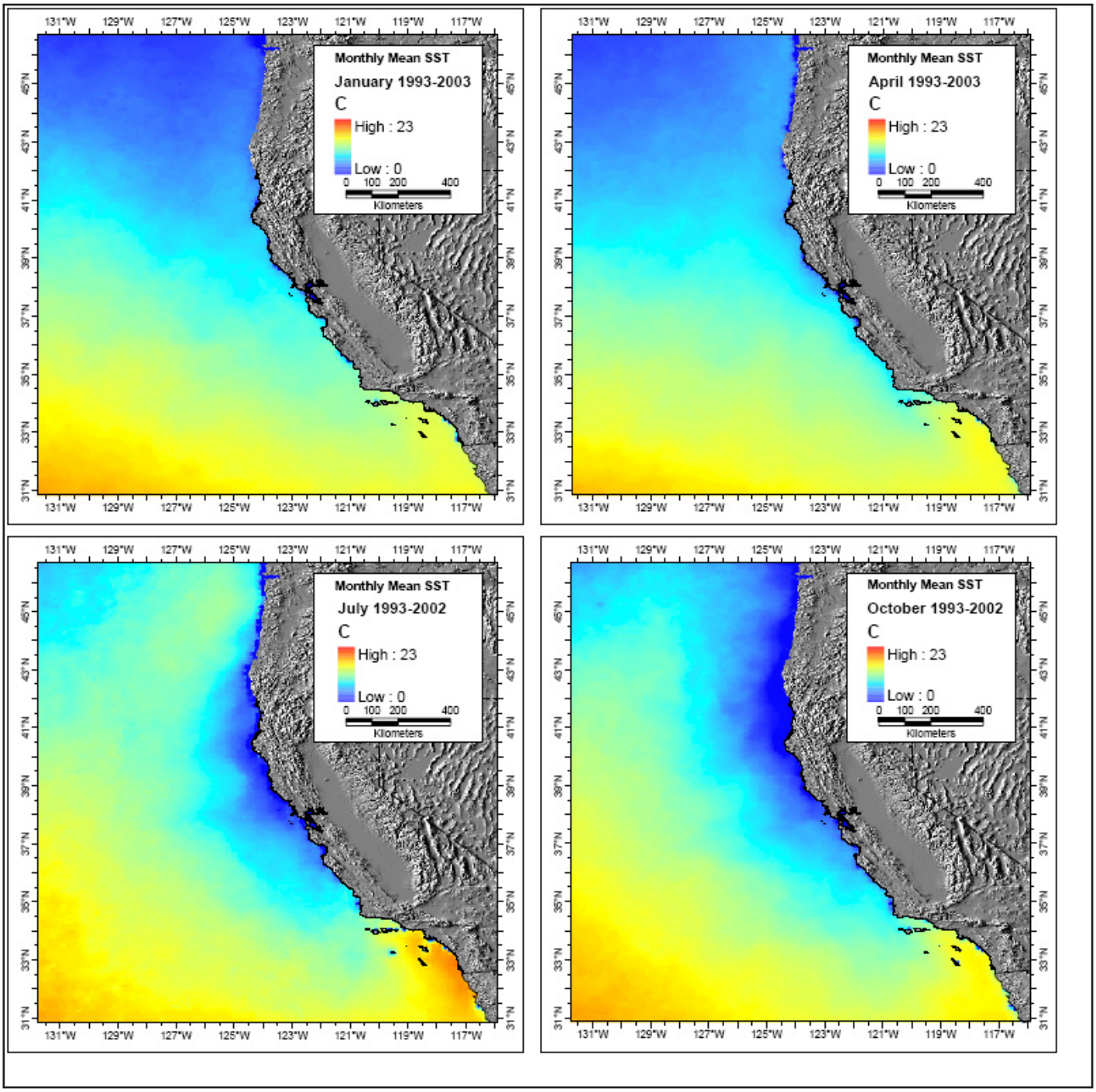

Figure 2.7.1. Seasonal mean sea surface temperature (January, April, July, and October) averaged across years from 1993 to 2003.

70,000 km^2, approximately 2% of the analysis area. Most the high area was confined to the coastline, with the largest area of frontal persistence observed in the area around the Channel Islands, most likely generated by the confluence of the cool south-bound California Current and warmer northbound Davidson Current. Frontal features extending along the northern California coast are generated by coastal upwelling events and the many eddies and gyres that spin out of the upwelling areas as they join the California Current.

Analysis of Boundary Concepts

The preceding discussion identified areas of high SST frontal persistence. Those areas closest to or within the current study area center around Sur Ridge, just south of Monterey Bay, and the Channel Islands. A total of 70% of the area contained within current CINMS boundaries was classified as having high SST frontal persistence. As such, it is important to note that the No Action Concept (NAC, current boundary) captures a large area of high frontal persistence.

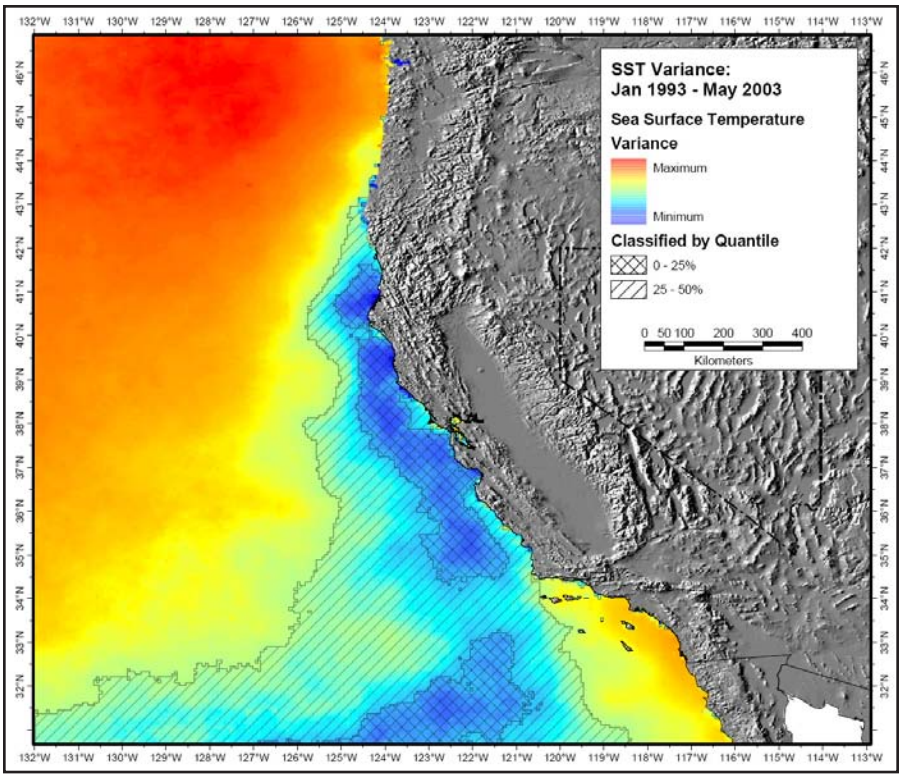

Figure 2.7.2. Sea surface temperature variance, calculated from mean monthly values for the period January 1993 to May 2003. Cool tones represent low SST variance and warm tones represent high SST variance. Hatched area represents the lowest two quantiles.

Mean SST frontal persistence for the NAC was calculated to be 29.6 months. Mean frontal persistence for the remaining concepts, ranging from smallest in size to largest are as follows: Concept 5-27.9 months; Concept 4-23.9 months; Concept 3-23.2 months; Concept 2-20.7 months; Concept 1a and 1-16 months. Mean frontal persistence for the study area boundary (defined in McGinnis, 2000) was estimated to be 19.4 months. Overall, mean SST frontal persistence decreases as area increases (Figure 2.7.6 and Table 2.7.1). Because the area of high frontal persistence is proportionally concentrated around the Channel Islands themselves, as additional areas away from the islands are included, less area of high frontal persistence is captured.

Due to the dynamic nature of SST and frontal boundaries, OAI statistics were not generated for the boundary concepts. However, it is important to note

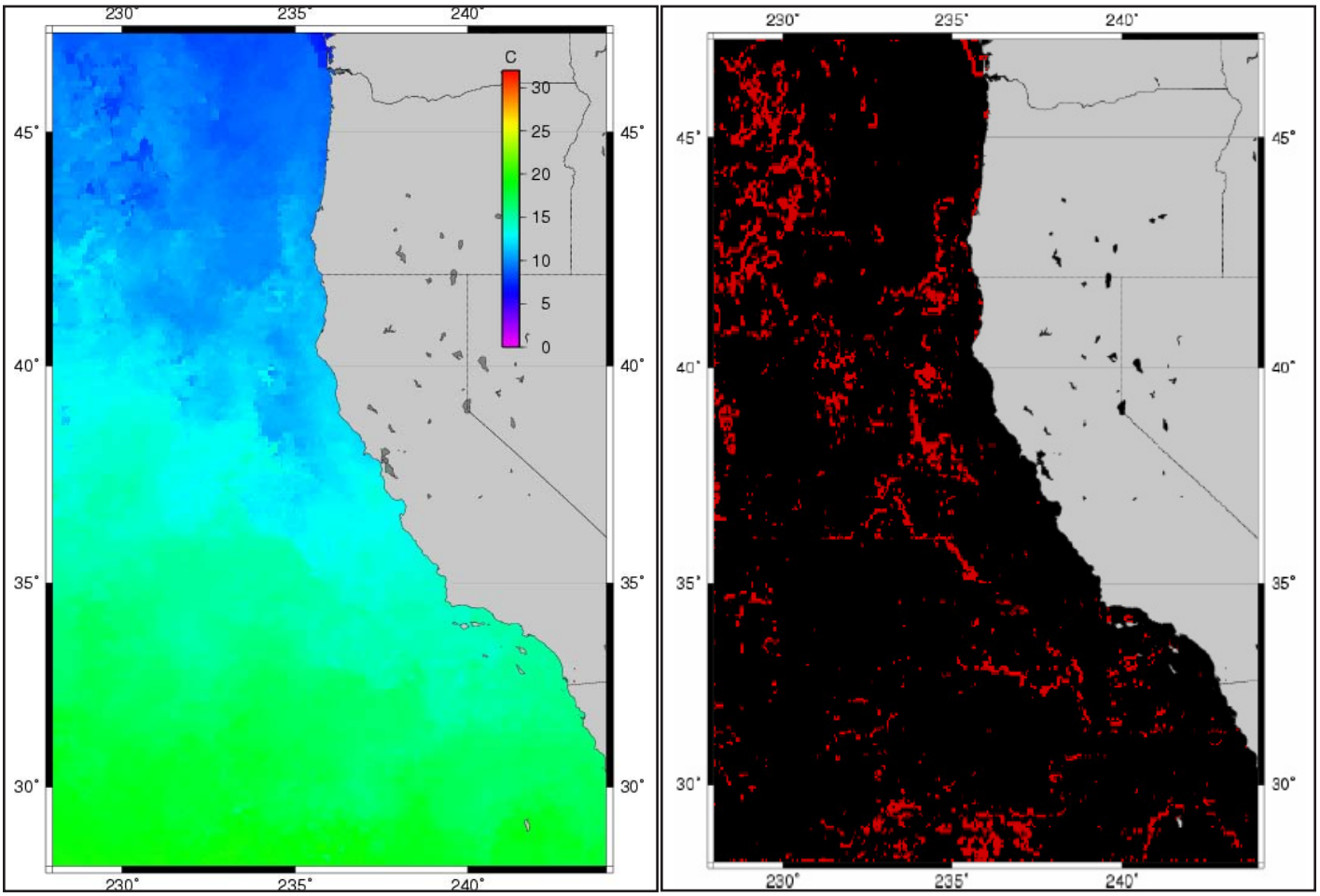

Figure 2.7.3. Left panel shows an example interpolated SST grid from GMT for January 1993. Right panel shows a grid clip of the highest quantile from the January 1993 slope magnitude grid. Red areas indicate the top 5% of values and represent the steepest temperature gradients and are used to identify SST fronts.

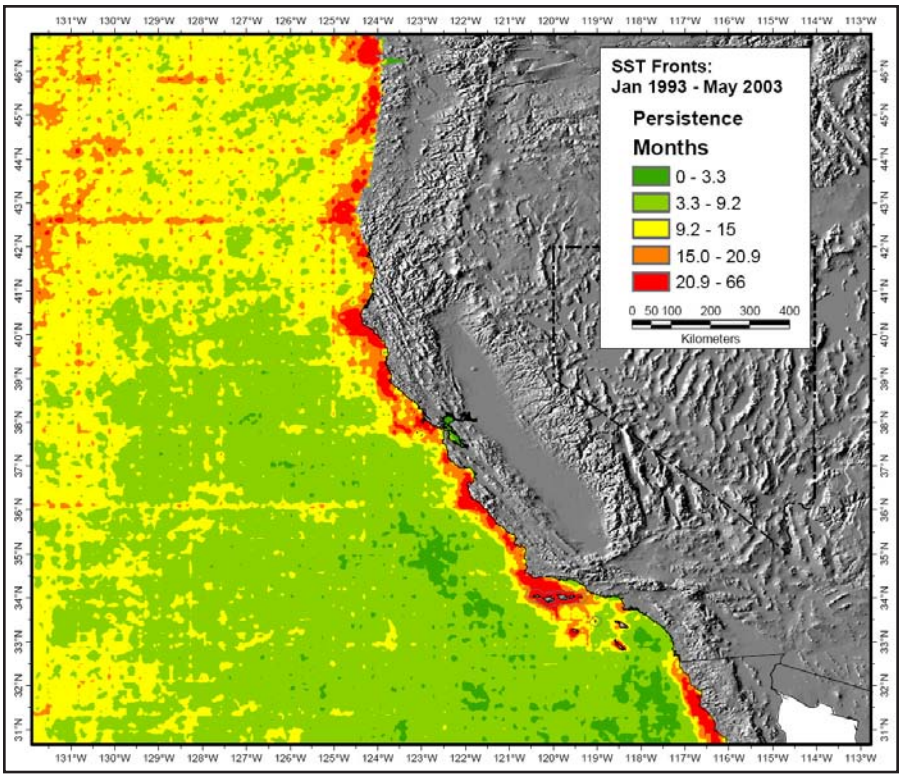

Figure 2.7.4. Persistence of SST fronts through time. Colors indicate number of months during which a front was evident, with green representing fewer months (1 std. dev. below the mean) to red (3 std. dev. above the mean).

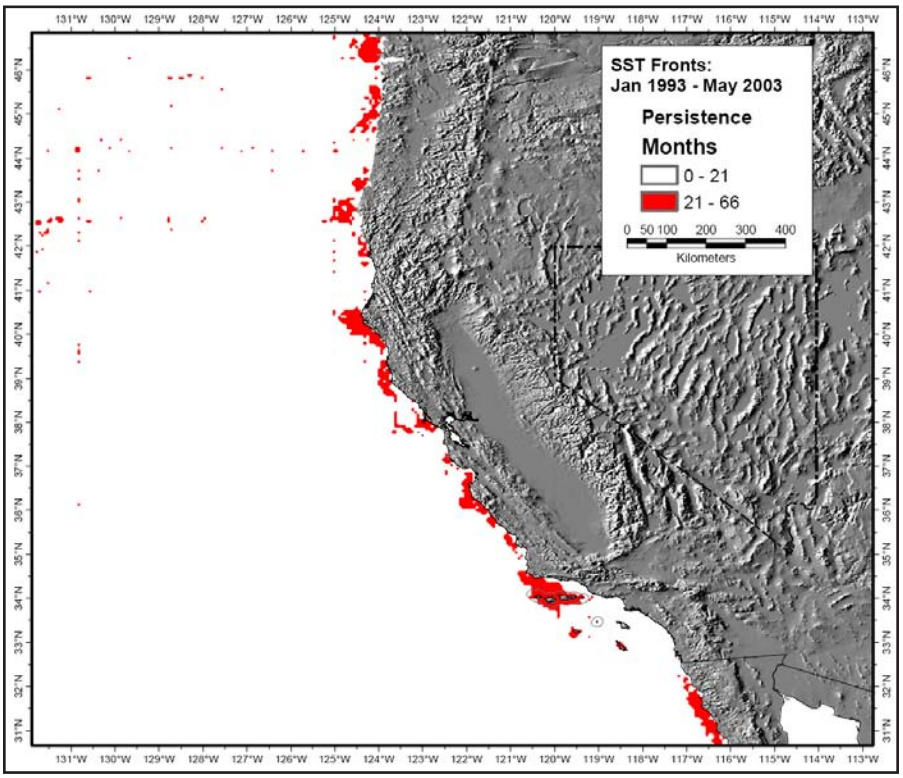

Figure 2.7.5. Areas with greatest SST front activity through time.

that since 1993 the area around the northern Channel Islands has been centered among a large area of SST front activity (Figure 2.7.5). In general, Figure 2.7.7 suggests that there is a point of dimishing returns with regard to additional area protected versus inclusion of more frontal activity (illustrated by the fitted polynomial equation). Concept 2 provides a large increase in SST frontal area, over Concepts 3, 4, and 5, relative to the total area of each. Concepts 1 and 1a, on the other hand, offer only a small increase in SST frontal activity over Concept 2 relative to additional total area.

Summary

• A stable area of sea surface temperatures exists along the California coast, ranging from California's northern border to Point Conception and extending offshore to 200 km.

• The Channel Islands National Marine Sanctuary encompasses a transition zone from cooler waters to the north and warmer waters to the south.

• A large portion of the current boundaries (~70%) include area identified as having persistent SST fronts. Concept 2 provides the greatest increase in persistent SST front area before returns begin to diminish (area of high SST frontal activity versus total area).

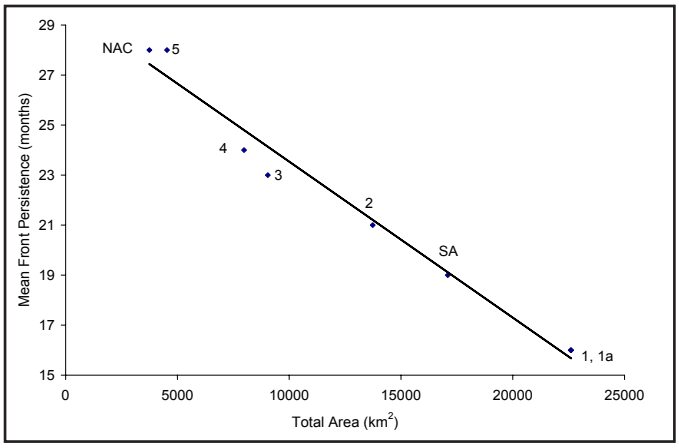

Figure 2.7.6. Linear regression function between concept area (km^2) and mean persistence of SST fronts.

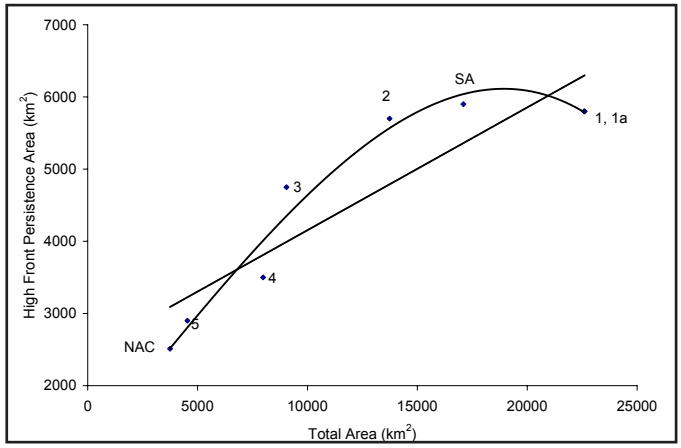

Figure 2.7.7. Linear regression function between total concept area (km^2) and area of high SST frontal persistence.

2.8 SURFACE CHLOROPHYLL AND OCEAN CURRENTS

Data and Methods

Pelagic marine food webs, including that of the Southern California Bight and adjacent waters, are supported by phytoplankton production. Throughout the year phytoplankton serve as a food source for protozoans, zooplankton, bivalves, and larval fishes (e.g., anchovies and sardines), which in turn are the foundation of a complex food web that supports all coastal fauna. Analyses of chlorophyll-a and currents presented here are intended to provide context for discussion in subsequent chapters on invertebrate, fish, bird, and mammal biogeography, and to lay the foundation for discussing interconnectivities between oceanographic processes and biogeographic patterns in the region.

The surface chlorophyll data presented here were derived from remotely sensed global chlorophyll-a concentration estimates (mg/m^3) acquired using the Sea-viewing Wide Field-of-view Sensor (SeaWiFS). The purpose of SeaWiFS is to provide quantitative data to resolve the magnitude and variability of chlorophyll concentrations, and subsequently to estimate primary production by marine phytoplankton. Presented here are level-3 processed data derived from the first 26 months of acquisition (November 1997-December 1999). This time period was selected because data for these months were readily available. Level 3 data consists of geophysical parameters binned to a 9x9 km (81 km^2) global equal-area grid at daily, 8-day, monthly, and annual intervals. Level 3 geophysical parameters consist of five normalized water-leaving radiances (radiance data corrected for atmospheric light scattering and sun angles differing from nadir), and seven geophysical parameters derived from the radiance data. This level categorization was developed by NASA to indicate that the data have been post-processed to contain both geophysical parameters and geographic coordinates.

In addition, to gain a broader understanding of the observed large-scale patterns in surface chlorophyll, estimates of surface current vectors, showing both magnitude and direction are also presented. Current data were derived using ocean surface altimetry collected by the ERS-2 and TOPEX/POSEIDON satellites. Monthly averaged current vectors were developed for identical months and years as described for ocean color, and have a horizontal resolution of 0.25 degrees (~28 km). When superimposed on ocean color, these vectors exhibit clear spatial correlations with patterns in observed chlorophyll concentrations, and are used, in part, to set the oceanographic context for subsequent analyses of ocean color and other biological resource distributions in the region. All data and analyses presented in this section were derived from data made available through the Marine Conservation Biology Institute's (MCBI) Baja California to Bering Sea Conservation Initiative (B2B). More information about MCBI and the Bering to Baja initiative can be found at <http://www.mcbi.org>.

To best achieve the study objectives of analyzing spatial patterns in relation to proposed boundary concepts, ocean color data for 26 months (November 1997-December 1999) were averaged to provide an estimate of mean chlorophyll-a concentration ([ChlA]) along the Pacific coast of the United States (ranging from 28°-49° latitude). Data from 2000 to present were available, however at the time of analysis these data were not post-processed and were not included. While ocean color is variable in all dimensions, a composite estimate (mean [ChlA]) was

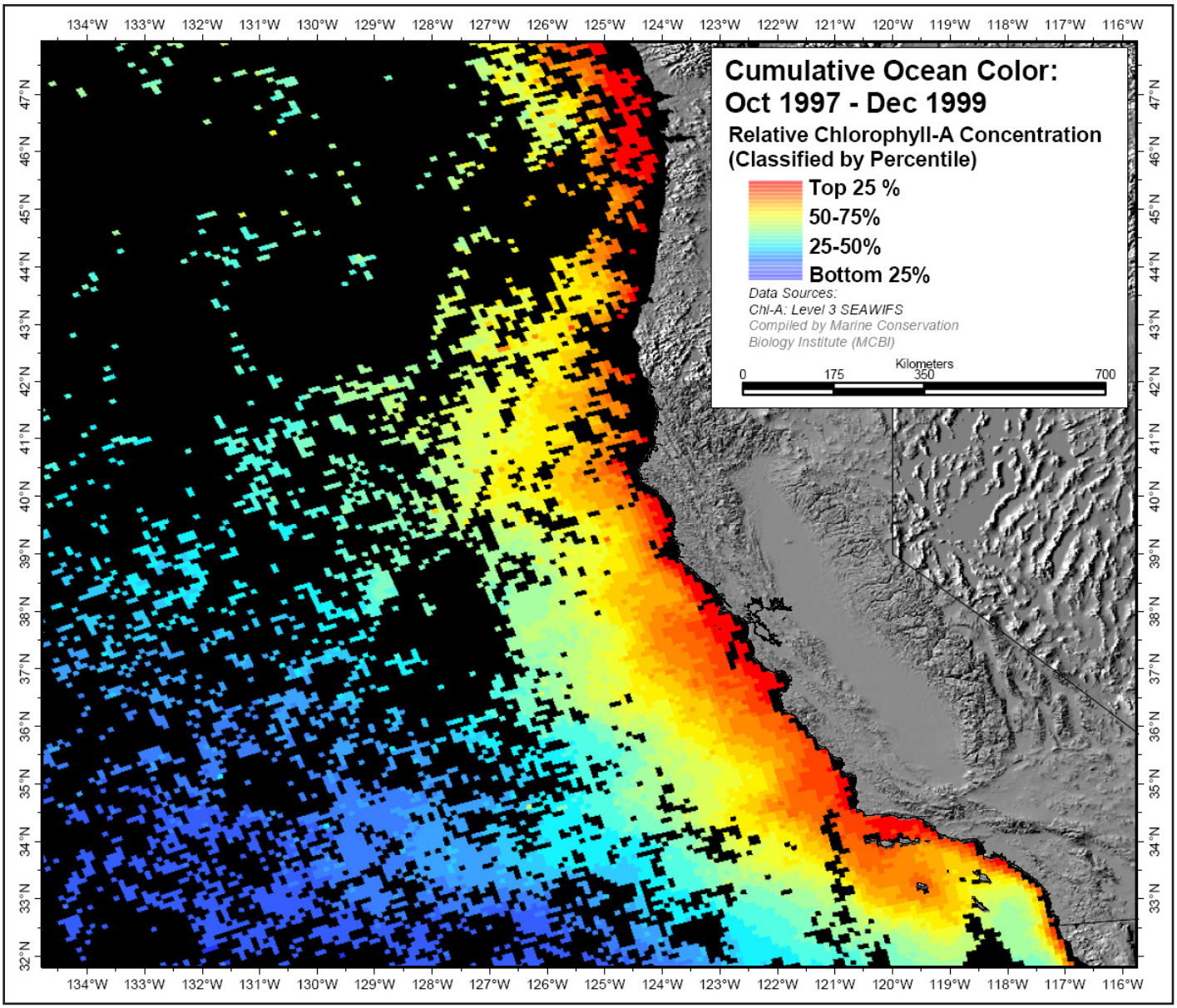

Figure 2.8.1. Average [ChlA] for grid cells in which data was present during November 1997-December 1999. Areas in black indicate grids cells where one or more months were not available. Warm tones indicate high mean [ChlA], while cool tones represent low mean

analyzed as CINMS boundaries will not change in response to monthly variation in oceanographic condition. An average concentration was calculated only for grid cells in which data were present during all 26 months (Figure 2.8.1). Excluding grid cells lacking full temporal coverage was done to minimize biases that may result from a disproportionate expression of seasonal [ChlA], thereby biasing the average value in that cell. Grid cells shaded in black indicate areas where one or more months were not available due to cloud cover, etc. Once calculated, mean values were then used to construct a model to estimate mean [ChlA] throughout the geographic extent using an interpolation technique (kriging) which resulted in a statistically smoothed raster surface (Figure 2.8.2).

To accomplish this, the calculated mean [ChlA] was first assigned to a point at the center of the cell (i.e. the cell centroid). These point data were then tested for significant spatial autocorrelation using the Moran's I and Geary's C statistics (Kaluzny *et al*., 1998). Significant autocorrelation indicates that points that are nearer to one another tend to have more similar values than points that are far away (Legendre, 1993), and is prerequisite to accurate interpolation. Next, the spatial autocorrelation was described using a variogram, which summarizes the decrease in relatedness between pairs of points as the distance between them increases. Parameters of the resulting variogram were used in the kriging procedure, which provides a surface of predicted values, as well as a standard error map indicating regions of confidence in the accuracy of estimated mean surface chlorophyll. To avoid displaying estimates of modeled surface chlorophyll in areas where we have little confidence, the standard error map was used to clip (mask) the interpolated surface. The resulting map (Figure 2.8.3) displays interpolated mean [ChlA] for those regions where the standard error was in the lowest 30 percent. The modeled accuracy

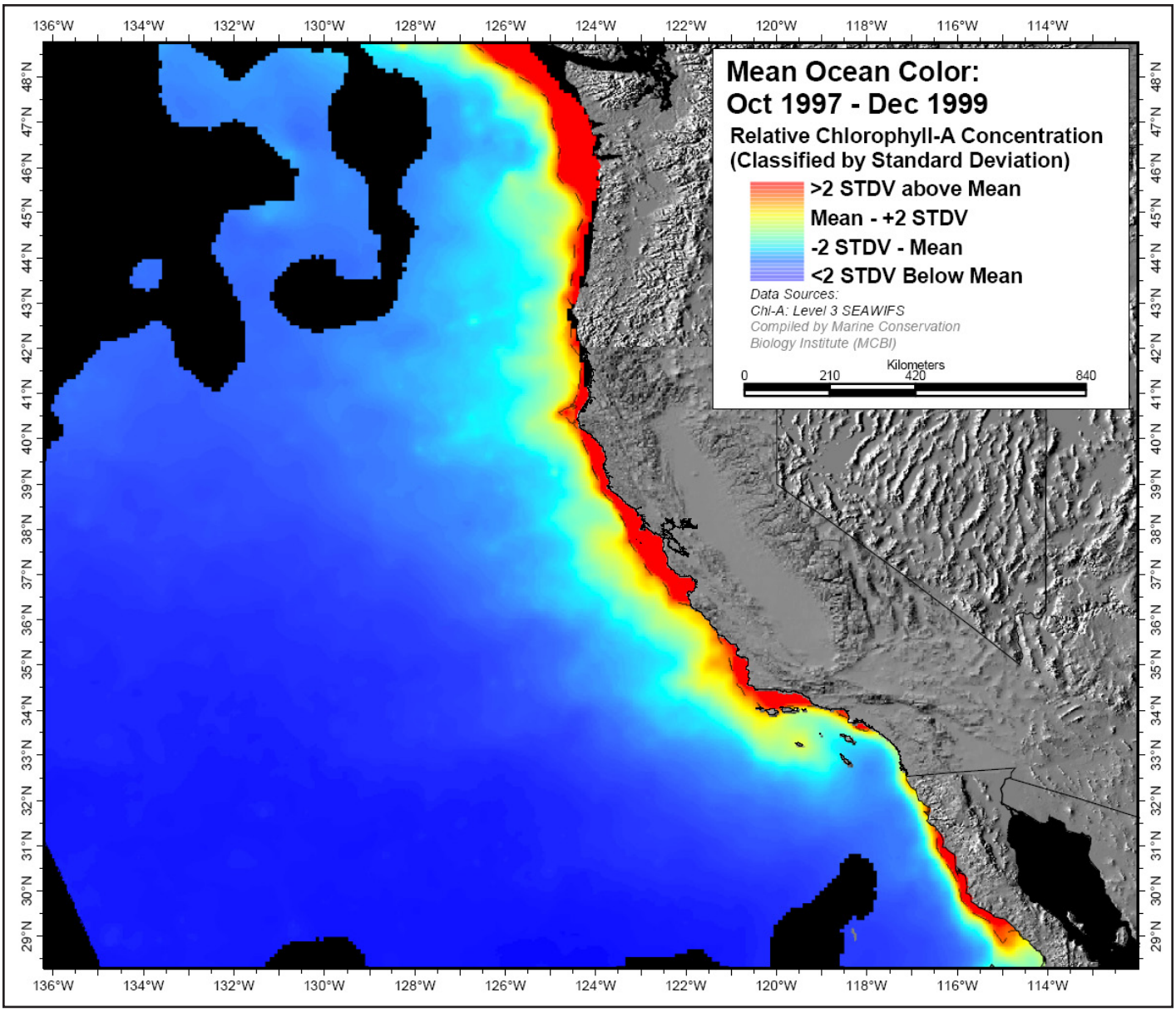

Figure 2.8.2. Interpolated mean chlorophyll concentration [ChlA] for the period between November 1997 and December 1999. Model extent ranges from 28°- 49°N. Warm tones indicate high mean [ChlA], while cool tones represent low mean [ChlA]. Areas clipped by the model standard error map appear black.

was then assessed using standard cross-validation techniques. Regressing predicted values against observed values yielded a coefficient of determination (r^2) of 0.97 ($p<0.001$).

Estimated patterns of ocean color should be interpreted with care, as they represent a composite of 26 months, some of which were considered by oceanographers to have taken place during a strong El-Niño period. As stated above, surface chlorophyll can be highly variable, and the average surface provided in this report is designed only to highlight areas of relatively persistent high [ChlA]. In addition to the mean [ChlA] map and analysis, mean monthly maps of surface chlorophyll and current vectors are also provided for 1999 (see broad-scale patterns below), but are not individually analyzed relative to the boundary concepts. 1999 was selected from the available years as it represents a relatively "normal" year in the El-Niño-Southern Oscillation (ENSO) cycle (Dandonneau *et al*., 2003).

Broad-scale Patterns

The interpolated 26-month mean surface chlorophyll model resulted in estimated concentrations of near-surface chlorophyll that were higher (warm tones) nearshore than offshore throughout the analysis extent (Figure 2.8.3). Stippled areas on the map indicate areas where average [ChlA] was greater than 2 standard deviations above the mean (henceforth "high"). A conspicuous area of high [ChlA] can be seen centered on the nearshore wa-

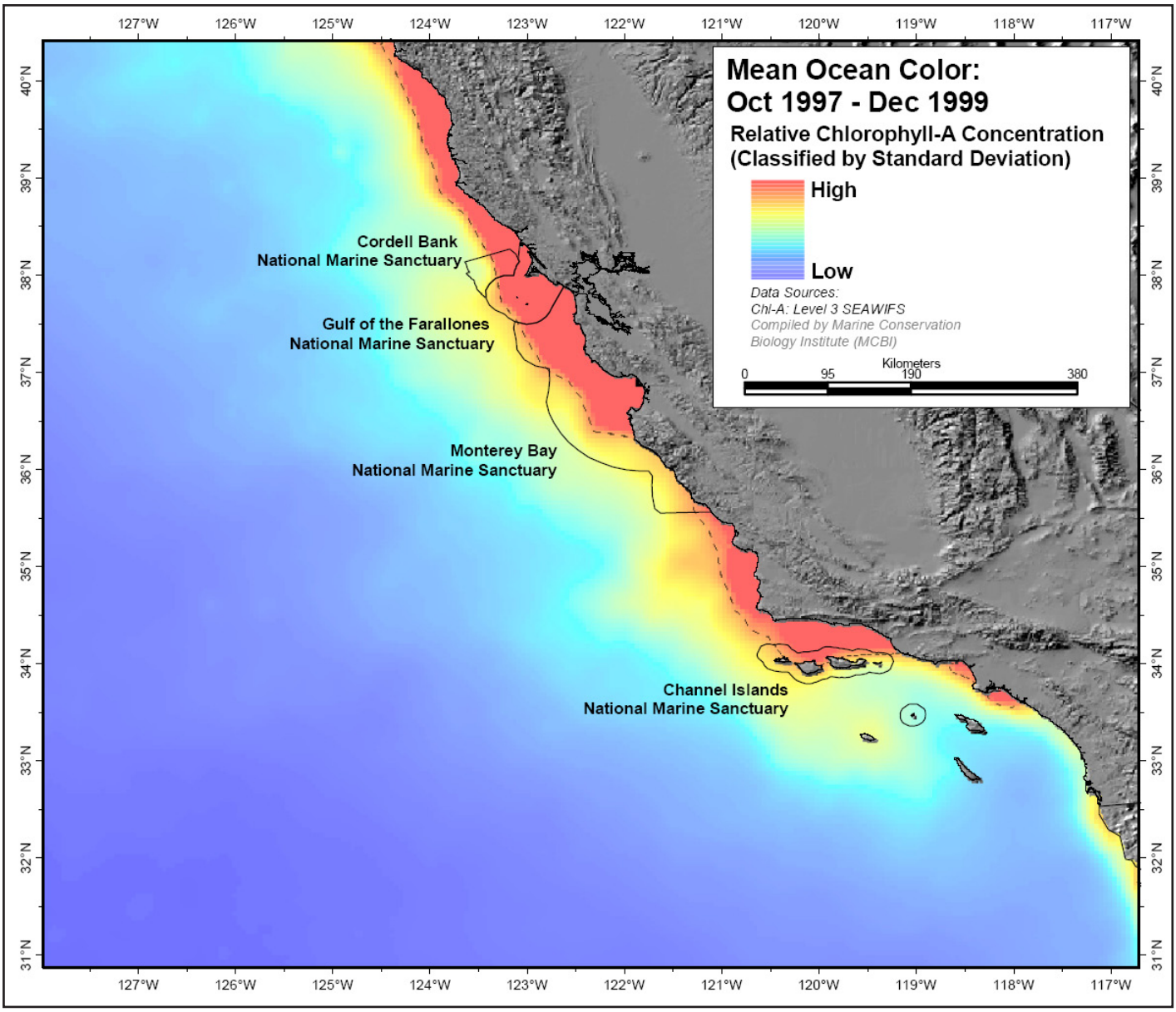

Figure 2.8.3. Interpolated mean chlorophyll concentration [ChlA] for the period between November 1997 and December 1999. Stippled areas on the map indicate where average [ChlA] was greater than 2 standard deviations above the mean. Warm tones indicate high mean [ChlA], while cool tones represent low mean [ChlA].

ters off Points Arguello and Conception, extending northward to Cambria, and eastward into the Santa Barbara Channel (SBC), settling into the Santa Barbara-Ventura Basin (refer to Figure 2.1.1). It is interesting to note that waters exhibiting relatively low [ChlA] can be found in the adjacent Santa Monica-San Pedro Basin which is deeper, and typically fed by warm, less nutrient-rich waters of the northward flowing California countercurrent. A second much larger area of high [ChlA] can be seen extending from just south of Monterey northward through the entire range of the analysis. In both cases, the seaward extension of elevated ocean color averages approximately 50 km, and then attenuates rapidly thereafter.

Two smaller areas of relatively high [ChlA] also can be seen just offshore of Santa Monica and Newport Beach; however, these are likely expressions of nutrient enrichment resulting from allocthonous materials sent downstream of the Santa Anna River, and San Mateo, Malibu, and various other creeks. This may be further exacerbated by agricultural and urban runoff from the densely populated Los Angeles basin. As such, high [ChlA] is clearly not always a sign of a healthy marine environment. Nutrient enrichment (eutrophication) can lead to hypoxia which has the propensity to profoundly affect an ecosystem, and cause physiological stress to associated aquatic organisms. The Committee on Environment and Natural Resources (CENR) released a report in 2003 which indicated that fertilizers and point source pollutants contribute the majority of nitrogen that is exported to marine and estuarine ecosystems in the southern California region (CENR, 2003). As such, it is not surprising to see this expressed in our analysis.

Results also indicate that the complement of sanctuaries along the California coastline (Gulf of the Farallones, Cordell Bank, Monterey Bay, and Channel Islands) captures substantial areas of high estimated mean [ChlA]. In this analysis (ranging from 28° to 49° latitude), the total area identified as high [ChlA] was 97,584 km^2. Roughly 11,728 km^2 (~11%) of this high area is contained within the four California Sanctuaries. Roughly 1% of the high area fell inside the boundaries of the Channel Islands National Marine Sanctuary (NAC). However, this represents 24% of the area contained within current CINMS boundaries. This is the smallest proportion of any California sanctuary (Gulf of the Farallones-85%, Monterey Bay-53%, and Cordell Bank-43%).

Highest phytoplankton biomass in the region has generally been reported to occur in nearshore surface waters, with maxima most frequently occurring during the spring and summer upwelling season when nutrient content of surface waters is relatively high (Airamé *et al*., 2003a). Spatial and temporal trends in ocean color shown here corroborate these findings, with monthly mean [ChlA] maps for 1999 suggesting that peak phytoplankton concentrations occurred between March and June of that year (Figures 2.8.4 and 2.8.5a). Additionally, current vectors suggest that the spatial patterns in [ChlA] are largely controlled by geostrophic flow. This can be clearly seen during the summer months where current jets and filaments can be seen transporting phytoplankton offshore. Thus, many of the region's biological resource distributions are influenced by these surface currents, and by other larger-scale ocean currents such as the southward flowing California Current and northward flowing southern California Countercurrent. This notion is not new, as many scientists have published their findings on the interrelationships between marine fauna and local oceanographic climate (Oedekoven *et al*., 2001; Ainley *et al*., 1994; Allen, 1994; Briggs *et al*., 1987; and Chelton *et al*., 1982).

The current vectors provided here (Figures 2.8.5a,b) reveal the persistent cyclonic flow pattern discussed in section 2.3. These surface currents can be seen during each month south and west of Point Conception. This pattern of surface circulation meandered only slightly through the duration of 1999. It is interesting to note that during the spring and early summer, an anti-cyclonic flow pattern set up along coastal waters centered on Morro Bay. These counter-rotating flows were presumably the result of the convergence of the California Current and southern California Countercurrent. This dynamic system of eddies, gyres, jets, and filaments clearly impact the distribution of observable phytoplankton distribution.

Analysis of Boundary Concepts

The preceding discussion identified a large region of high mean [ChlA] centered on Points Arguello and Conception, ranging from Cambria in the north southward along the shelf to Point Conception, where it then spreads eastward throughout the entire Santa Barbara-Ventura Basin. A total of 24% of the area contained within current CINMS boundaries was classified as having high [ChlA]. As such, it is important to note that the No Action Concept (NAC, current boundary) is reasonably well configured to capture areas of high [ChlA], and a review of the remaining concepts suggests that only boundary concepts 2 and 5 provide viable options in terms of optimizing expansion to capture areas of relatively high average primary productivity (Table 2.8.1). As discussed in Chapter 1.4, two Optimal Area Index (OAI) values are presented here. The first of which is calculated using the mean [ChlA] inside each of the concepts (henceforth "relative OAI"), and the second is calculated using the total area of high [ChlA] captured inside each boundary (henceforth "absolute OAI").

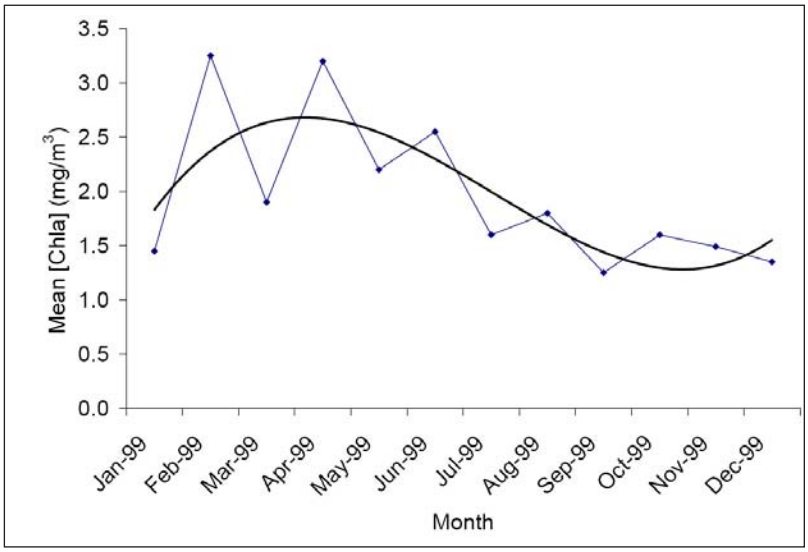

Figure 2.8.4. Monthy mean [ChlA] for 1999. Estimates derived from data contained within the Study Area boundary. Smooth line indicates a third-order polynomial through the observed estimates.

Mean estimated [ChlA] for the NAC was calculated to be 1.22 with a coefficient of variation (CV) of 23.3%. Mean diversity and CV values for the remaining concepts, ranging from smallest in size to largest are as follows: Concept 5-1.23, 24.3%; Concept 4-1.15, 29.0%; Concept 3-1.18, 30.4%; Concept 2-1.26, 29.3%; Concept 1a-1.22, 30.3%; and Concept 1-1.22, 30.3% (Figure 2.8.6). Mean [ChlA] for the study

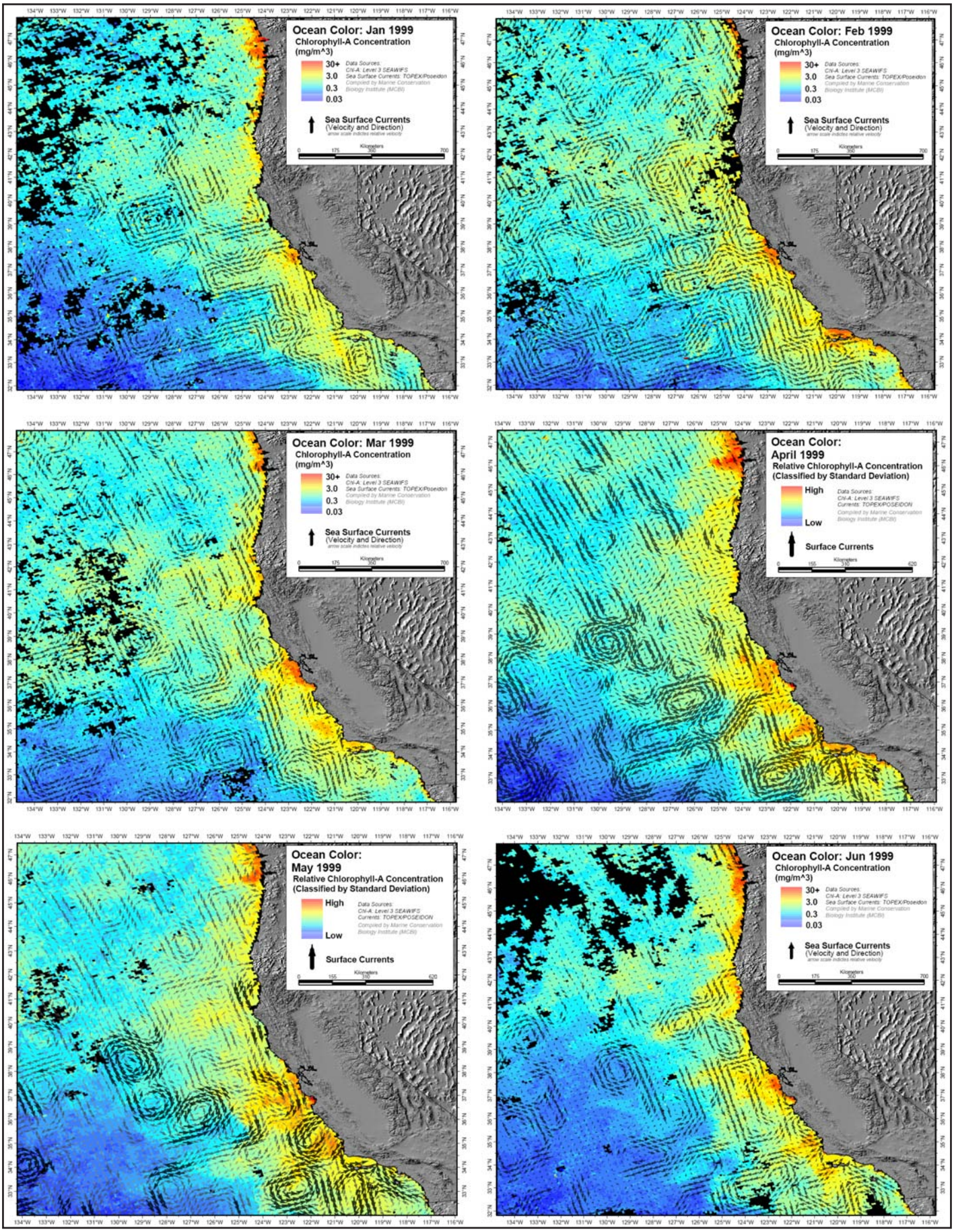

Figures 2.8.5a. Mean chlorophyll concentration [ChlA] for the months January to June 1999 (left to right). Altimetry derived surface current velocity vectors for the same time periods are superimposed on the [ChlA] surface. Large arrows indicate relatively strong flow (greater than mean), while small arrows indicate weak flow.

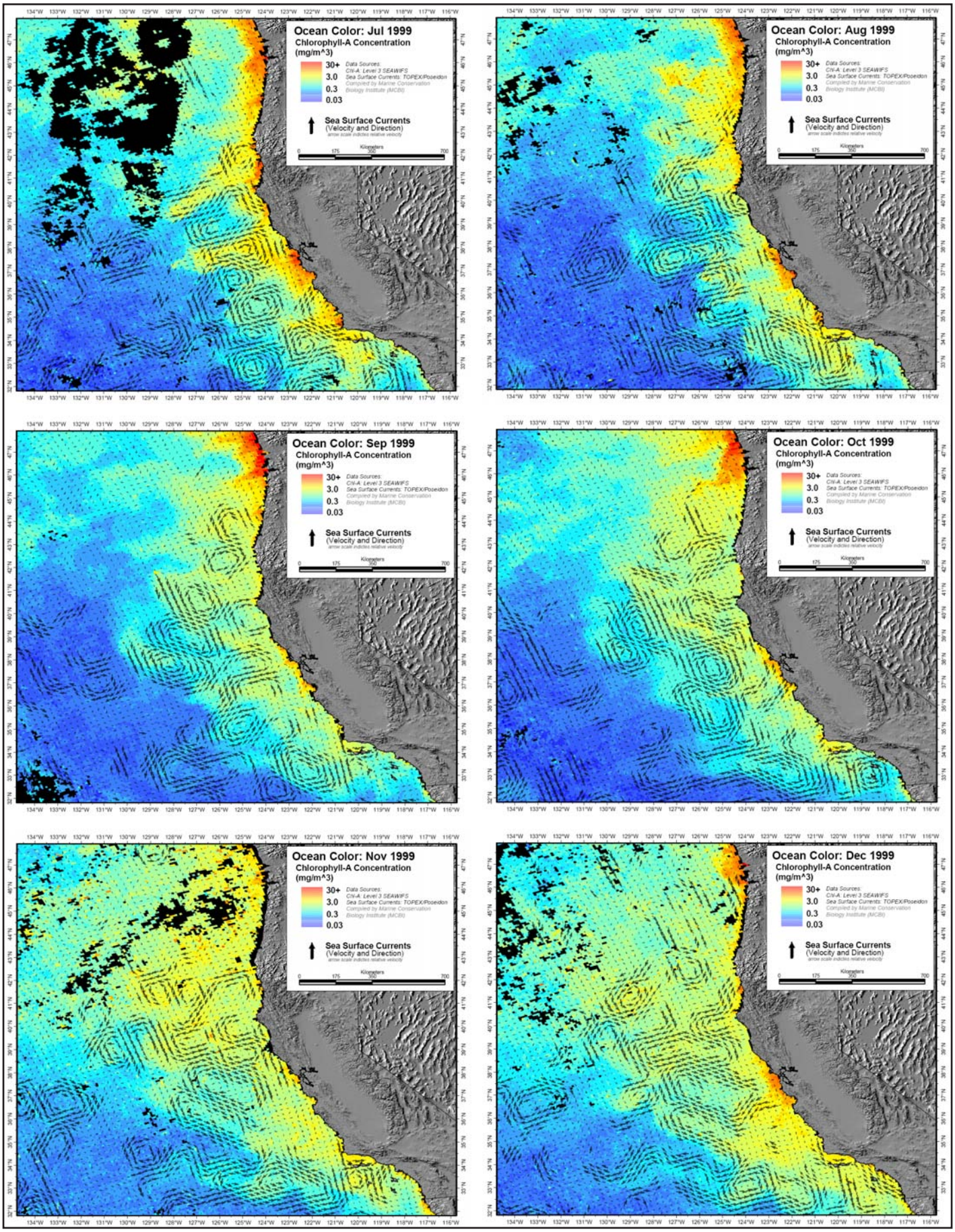

Figures 2.8.5b. Mean chlorophyll concentration [ChlA] for the months of July to December 1999 (left to right). Altimetry derived surface current velocity vectors for the same time periods are superimposed on the [ChlA] surface. Large arrows indicate relatively strong flow (greater than mean), while small arrows indicate weak flow.

area boundary (defined in McGinnis, 2000) was estimated to be 1.29 with a CV of 30.3% (Figure 2.8.6). Of the concepts in question, only 2 and 5 exhibited a higher mean [ChlA] value than the NAC (Table 2.8.1). It is important to note that the Study Area also resulted in a high relative OAI, but is not currently under consideration as a concept. These results show no statistical relationship to concept size, unlike the predictable relationships discussed in chapter 1.4. This lack of trend is shown in Figure 2.8.7 as a linear regression function between concept area (km^2) and the mean [ChlA] value calculated within the boundary (r^2=0.07, P=0.45). The relationship between concept area and absolute area of high [ChlA] is very predictable (and statistically significant), with larger concepts containing ever larger areas of high [ChlA]. Figure 2.8.8 shows the linear regression function between the total concept area (km^2) and the area of high [ChlA] contained within the boundary (r^2=0.99, P<0.0001).

A more balanced metric to use in assessing the relative benefits of each concept as it relates to optimizing for high [ChlA] is the OAI (Table 2.8.1). While this metric decouples the predictable relationships between concept area and the relative and/or absolute estimate to some extent, results of the OAI are still dependent upon the input data – absolute vs. relative measures. As such, we've provided results of the OAI for both mean and area of high [ChlA]. Again, the OAI takes into account the proportional (%) change in [ChlA] as you step from the NAC to each of the concepts under consideration. It also incorporates the proportional change (%) in area from the NAC. Results suggest that Concept 5, the minimum expansion concept, provides maximum benefit in terms of the mean [ChlA] calculated for each concept (relative OAI), while concept 2 provides the highest absolute OAI value in terms of the area of high [ChlA] contained within each concept. Because the mean OAI incorporated a negative value in the numerator for concepts 1, 1a, 3, and 4 (decreased [ChlA]), the calculated value is necessarily negative.

Table 2.8.1. Analysis of chlorophyll within boundary concepts. Numbers in bold indicate an increase in the estimate when compared to the No Action Concept (NAC). Maximum calculated OAI numbers are shaded in gray. Delta (Δ) indicates a rate of change calculation, and is always expressed as a percent change from the NAC.

Concept	Area (km^2)	Mean ChlA	High ChlA Area (km^2)	Δ Area (%)	Δ Mean ChlA (%)	Δ High ChlA Area (%)	Mean ChlA OAI (relative)	High ChlA Area OAI (absolute)
NAC	3745	1.223	981	-	-	-	-	-
5	4536	1.233	**1225**	21.12	0.82	24.87	0.39	1.178
4	7981	1.146	**2056**	113.11	-6.30	109.58	-0.056	0.969
3	9044	1.176	**2683**	141.50	-3.84	173.50	-0.027	1.226
2	13736	**1.263**	**4842**	266.78	3.27	393.58	0.012	1.475
1a	22591	1.215	**6437**	503.23	-0.65	556.17	-0.001	1.105
1	22613	1.215	**6414**	503.82	-0.65	553.82	-0.001	1.099
SA	*17093*	*1.291*	*6441*	*356.42*	*5.56*	*556.57*	*0.016*	*1.562*

Summary

• Patterns of mean [ChlA] show highest concentrations in nearshore waters during spring and summer, and in some cases, appear in locations known for upwelling.

• Patterns of mean [ChlA] are clearly related surface current patterns.

• Of the boundary concepts under consideration, Concepts 2 and 5 provide relatively large increases in [ChlA] for their size in comparison to the NAC.

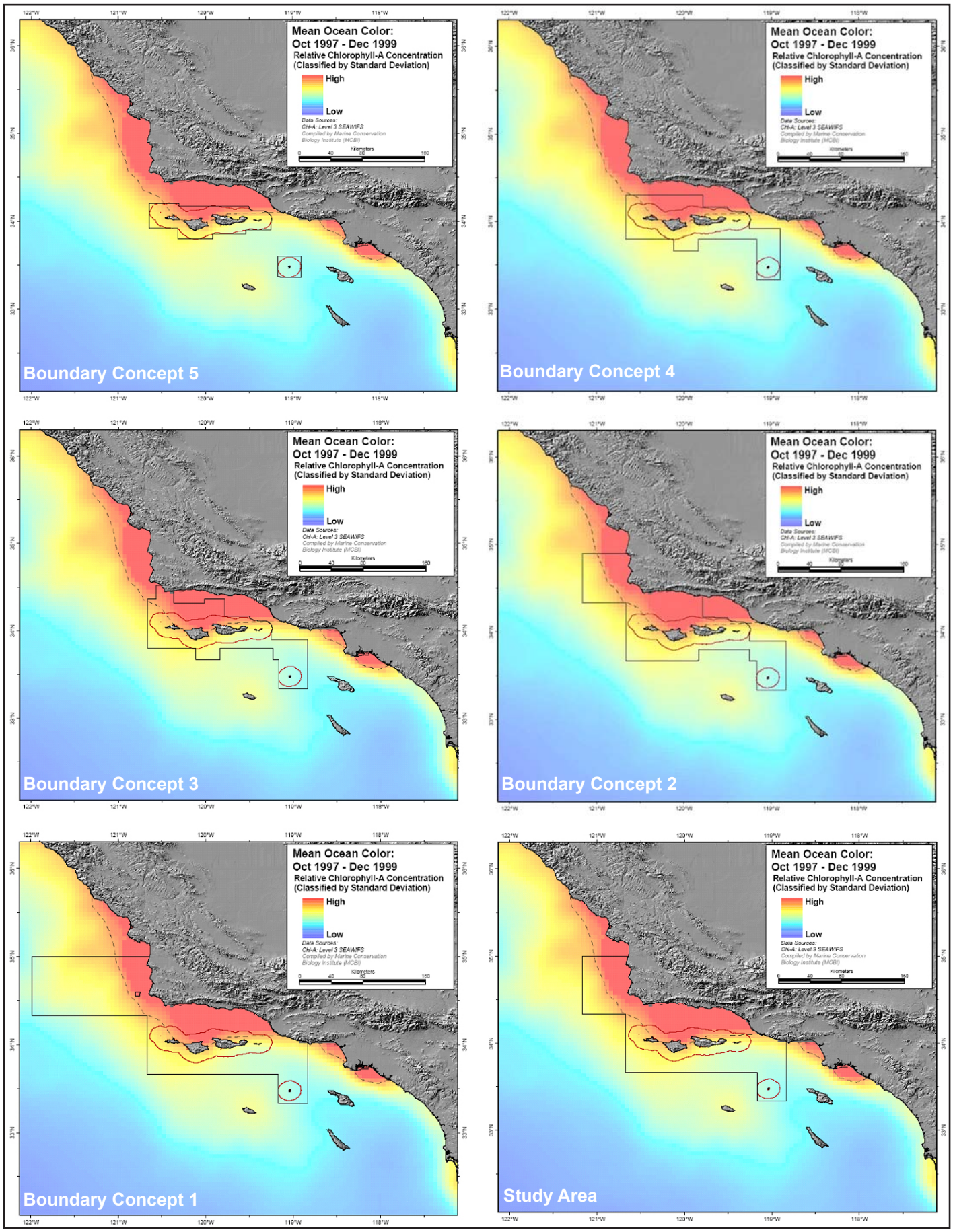

Figure 2.8.6. Interpolated mean chlorophyll concentration [ChlA] for the period between November 1997 and December 1999 with boundary concepts overlain. The No Action Concept (NAC) is shown as a red line, while the concepts are shown as a black line.

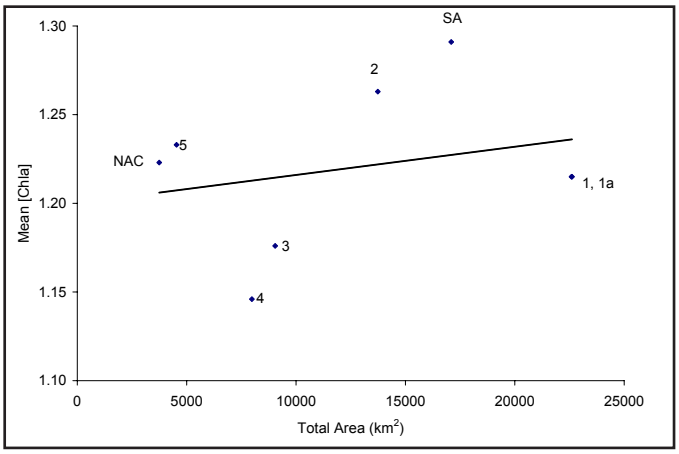

Figure 2.8.7. Linear regression function between concept area (km^2) and mean [ChlA].

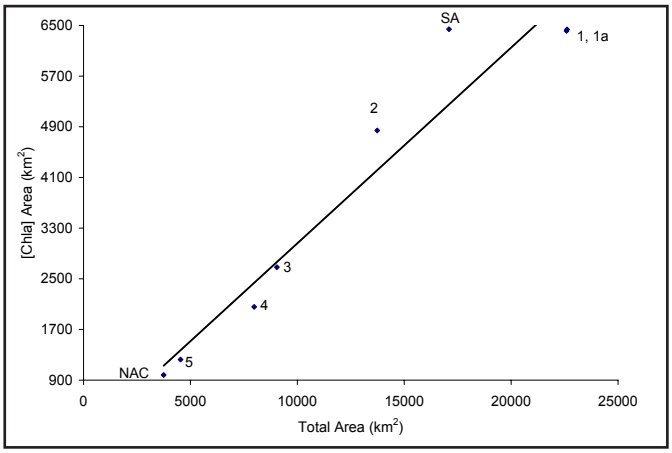

Figure 2.8.8. Linear regression function between the total concept area (km^2) and area of high [ChlA].

2.9 SUBMERGED AQUATIC VEGETATION DISTRIBUTION: EELGRASS AND SURFGRASS

Data and Methods

Data presented here are a compilation of all currently available quality controlled submerged aquatic vegetation (SAV) GIS data sets for the west coast of the United States, ranging from 33° to 49° north latitude. The data were compiled from seventeen data sources. These sources were acquired over a large range of time periods, collected at several different spatial resolutions, and were collected using a variety methods, including: 1) aerial photography, 2) videography, 3) multispectral sensors, 4) sonar, and 5) standard field surveys. The temporal range of data used in this composite view of SAV is from 1987 through 2003. Data were originally developed for the Pacific States Marine Fisheries Commission in cooperation with the National Marine Fisheries Service (NMFS) Northwest Region and the Pacific Fishery Management Council to support the designation and conservation of Essential Fish Habitat (EFH) for Pacific Coast groundfishes. Data were consolidated and integrated in a GIS format to support spatially explicit habitat modeling and impact assessment on a coast-wide scale.

This SAV dataset was developed by TerraLogic GIS, Inc., and was published in April 2004. Data developers urge caution when analyzing and interpreting the data, as they merely represent a regional (*i.e.*, not persistent through time) view of SAV locations. It is also important to note that the distribution of SAV's can be quite ephemeral. Areas without mapped SAV may contain seagrass; however, digital data were unavailable during this data compilation. To analyze distributions of SAV in relation to proposed concepts, the total area of SAV was estimated within each boundary. The area calculated represents combined areas of Eelgrass (*Zostera marina*) and surfgrass (*Phyllospadix* spp.).

Z. marina occurs from Alaska to Baja California along the Pacific coast of North America. Eelgrass beds are generally considered to be extremely productive habitats that support a rich assemblage of fish species, and provide refugia for the larval and juvenile stages (Valle *et al*., 1999; Leet *et al*., 2001). Eelgrass habitat also is an important resource for birds, as it has an associated rich benthic faunal community that provides forage species for waterfowl and other marine birds. In California's bays and estuaries north of Monterey Bay, eelgrass also provides spawning habitat for Pacific herring (*Clupea pallasii*). Subsequently, birds such as scooters (*Melanitta* spp.), bufflehead (*Bucephala albeola*), and goldeneyes (*Bucephala clangula*), eat eggs deposited onto eelgrass by *C. pallasii* during the mid-winter spawn. In addition, birds such as surface-feeding ducks and the black brant (*Branta nigricans*) feed directly on eelgrass (Leet *et al*., 2001). Surfgrass (*Phyllospadix* spp.) is also considered to be a highly productive living habitat that provides shelter and resources for a variety of taxa (Stewart and Myers, 1980), including many fishes and invertebrates, such as the California spiny lobster (*Panulirus interruptus*) (Engle, 1979).

Because SAV's provide critical habitat for such a wide range of biological resources, the assumption of this analysis was that boundaries which encompass a larger area of SAV habitat are preferred, and that any addition of this habitat provides the potential for increased habitat and biological diversity. The total area of SAV habitat within each concept was then used in calculating an Optimal Area Index (OAI). Because estimates of SAV den-

sity, standing stock, or biomass were unavailable (only the estimated area and distribution were available), only results of the absolute OAI are provided (see Section 1.4 for further discussion on OAI).

Broad-scale Patterns

SAV distribution along the California coastline is patchy and discontinuous, with long stretches of the central coast – from San Francisco Bay south to Morro Bay – generally lacking significant areas of coverage (Figure 2.9.1). It is important to note that the polygons that portray SAV distribution in this map have been greatly exaggerated so that they can be seen at this scale. Data indicate that *Zostera* can be found throughout the range of this analysis, while *Phyllospadix* is generally more abundant south of Point Arguello. Leet *et al*. (2001) reported that SAV's are found to some degree in all of California's larger bays and estuaries, including Humboldt Bay, Tomales Bay, San Francisco Bay, Monterey Bay, Morro Bay, and San Diego/Mission Bay. Furthermore, SAV's are well established in several smaller open estuarine embayments along the coast. Maps presented here corroborate these reports.

In all, a total of 317 km^2 of SAV was mapped along the entire Pacific coastline of the coterminous U.S. Maps indicate that the complement of National Marine Sanctuaries along the California coastline (Gulf of the Farallones, Cordell Bank, Monterey Bay, and Channel Islands) do not capture large areas of SAV. Of the four California sanctuaries, only the Gulf of the Farallones and Channel Islands capture measurable areas of SAV. Gulf of the Farallones NMS contains approximately 22 km^2 (~7% of total mapped), while the CINMS contains approximately 19 km^2 (~6% of total mapped). Of these two sanctuaries, only the Channel Islands contained both *Zostera marina* and *Phyllospadix* spp.

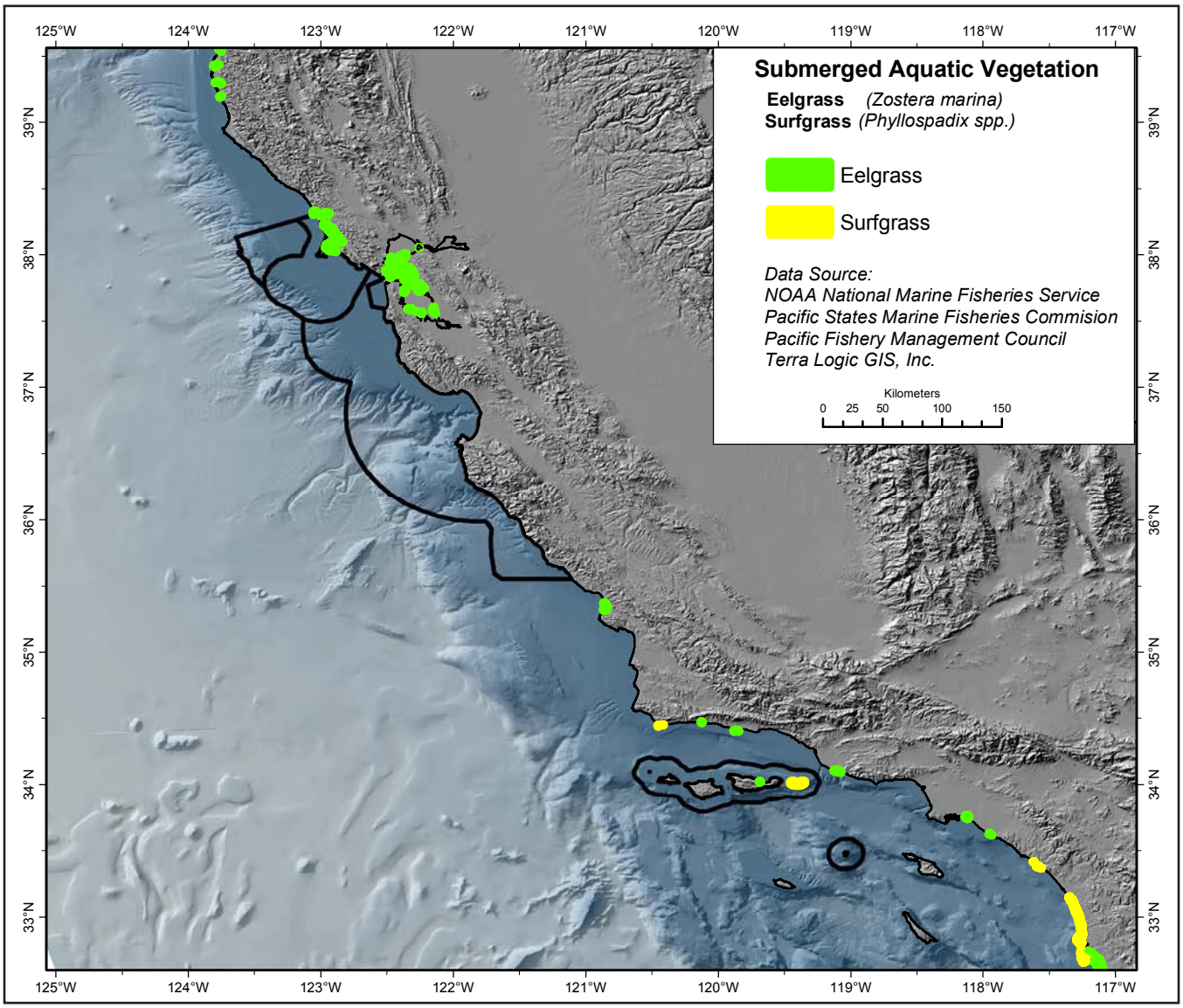

Figure 2.9.1. Distribution of submerged aquatic vegetation within coastal California waters.

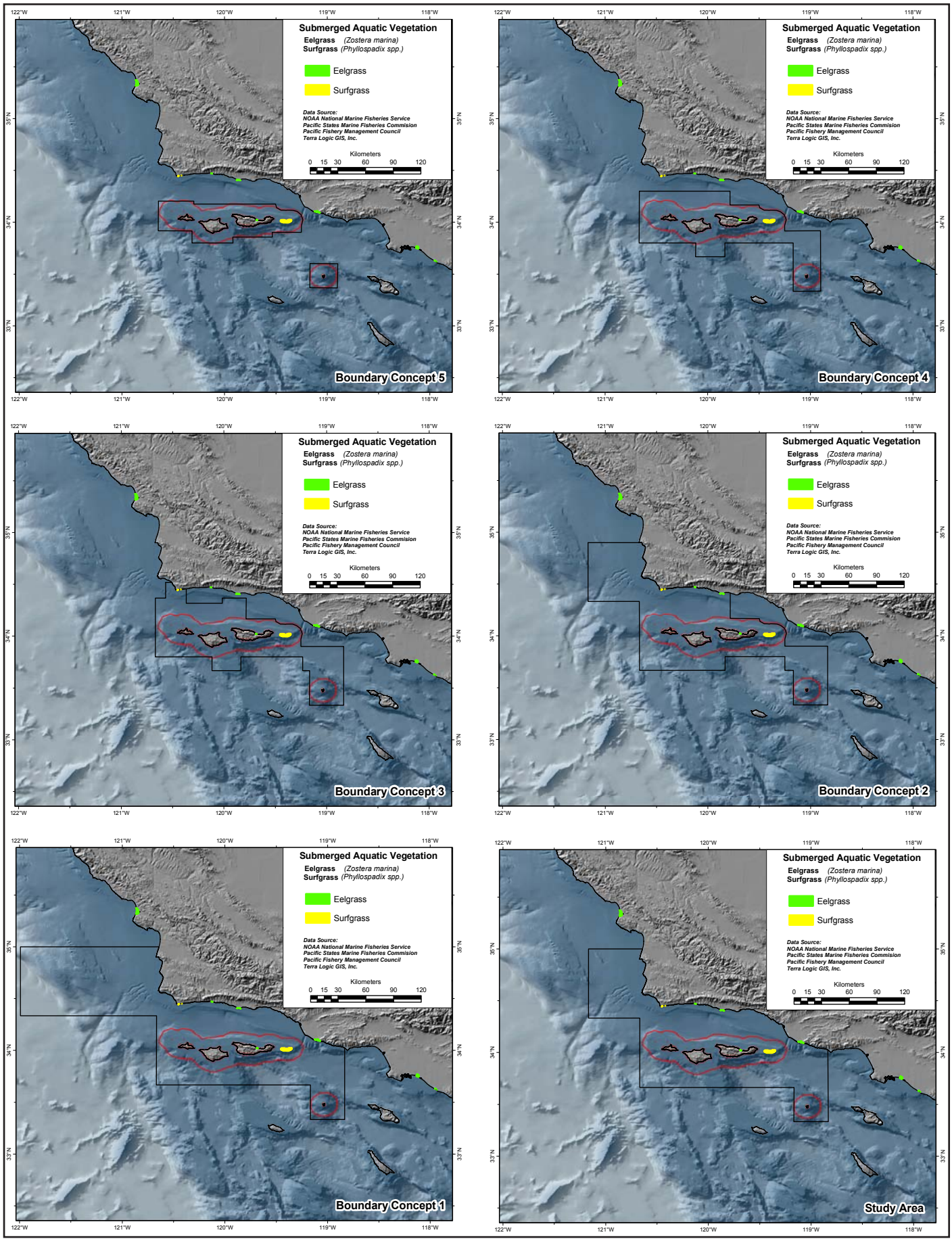

Figure 2.9.2. Distribution of submerged aquatic vegetation within the proposed boundary concepts in southern California.

Analysis of Boundary Concepts

While the total area of SAV within the current sanctuary boundary is modest (Table 2.9.1), it contributes approximately 46% of the total SAV beds contained within National Marine Sanctuaries along the California coast. Concepts 1, 1a, and 2 would encompass an additional 0.41 km^2, as would the study area boundary. This amounts to a 2% increase in area of SAV for concepts 1, 1a, and 2. Concept 3 would capture an additional 0.11 km^2, or an increase of 0.5%. Figures 2.9.2 show the distribution of SAV beds relative to each boundary concept. Results exhibit a predictable and statistically significant positive relationship to concept size (at a=0.05). This relationship is shown in Figure 2.9.3 as a linear regression function between concept area (km^2) and the area of SAV contained within each concept (r^2=0.83, P=0.001).

Table 2.9.1. Analysis of SAV distribution within boundary concepts. Numbers in bold indicate an increase in the estimate when compared to the No Action Concept (NAC). OAI estimates shaded in gray represent maximum observed benefit. Delta (Δ) indicates a rate of change calculation, and is always expressed as a percent change from the NAC.

Concept	Area (km^2)	SAV Area (km^2)	Δ Area (%)	Δ SAV Area (%)	OAI (absolute)
NAC	3475	19.00	-	-	-
5	4538	19.00	21.12	0.00	0.000
4	7981	19.00	113.11	0.00	0.000
3	9044	**19.11**	141.50	0.58	0.004
2	13736	**19.41**	266.78	2.16	0.008
1a	22591	**19.41**	503.23	2.16	0.004
1	22613	**19.41**	503.82	2.16	0.004
SA	*17093*	*19.41*	*356.42*	*2.16*	*0.006*

The optimal area index (OAI) values suggest that concepts 3, 2, 1, and 1a all would result in a net benefit in terms of SAV distributions, and that concept 2 would provide maximum benefit. This is due to the fact that while concepts 1 and 1a are substantially larger, they contain no further SAV beds than what is captured in concept 2.

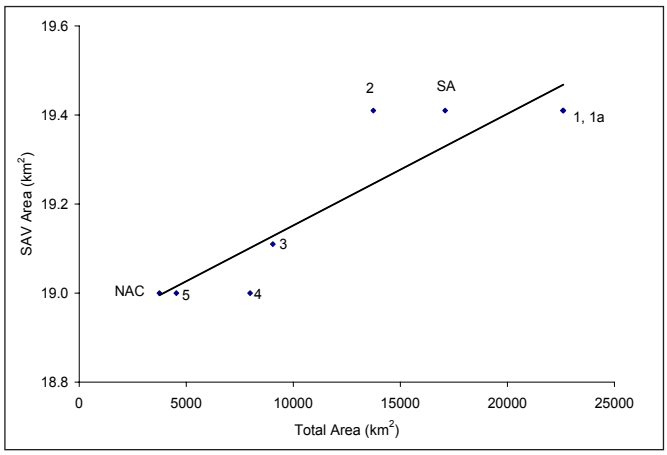

Figure 2.9.3. Linear regression function between area of SAV distribution and total area of boundary concepts.

Summary

- SAV distribution along the coast of California is patchy and discontinuous.
- The Channel Islands NMS presently contributes 46% of all mapped SAV beds contained within all four California sanctuaries.
- Of the boundary concepts under consideration, concept 2 provides relatively large increases in SAV area for its size.

2.10 KELP DISTRIBUTION

Data and Methods

Data presented here delineate kelp bed distribution (primarily *Nereocystis leutkeana* and *Macrocystis* spp.) along the coast of California, ranging from 32°-41° latitude. These data, developed by the California Department of Fish and Game (CDFG) Marine Region, are a subset of an entire west coast dataset that was used to support the National Marine Fisheries Service (NMFS) in the development of an environmental impact statement (EIS) that considers the designation of Essential Fish Habitat (EFH) for Pacific coast groundfish. Kelp data were digitized for use in a GIS from scanned aerial photos (1989 and 1999) and digital multispectral video data (2002). Assessments of accuracy for the abundance and distribution of kelp are uncertain due to the various sampling methods. Additionally, the strong association of kelp and the variability of oceanographic and climatic conditions may affect overall map accuracy. Therefore, kelp bed locations and extent may not reflect current or past conditions; however, the data are useful in identifying general patterns of kelp distribution and to highlight areas that have been known to support kelp growth. In this chapter, kelp data were analyzed to characterize its distribution along the coast of California and to compare spatial kelp coverage within the proposed boundary concepts.

Kelp forests provide habitat that supports a vast trophic web. Species of polychaetes, amphipods, decapods, gastropods, and ophiuroids are common among kelp holdfasts, while sponges, tunicates, anemones, cup corals, and bryozoans are frequently found under kelp canopies. Kelp also provides refuge for many species of young-of-the-year and juvenile fishes, such as señorita (*Oxyjulius californica*) and surfperch (*Brachyistius frenatus*), which are common throughout the canopy. Several species of rockfish are abundant in kelp forests: blue rockfish (*Sebastes mystinus*), olive rockfish (*S. serranoides*), and black rockfish (*S. melanops*). Furthermore, kelp forests provide a large source of prey for piscivorous birds, such as gulls, terns, snowy egrets, great blue herons, and cormorants. At the higher end of the trophic chain, many mammals seek prey items among the kelp structure, including: sea otters, harbor seals, and California sea lions (Airamé *et al*., 2003a).

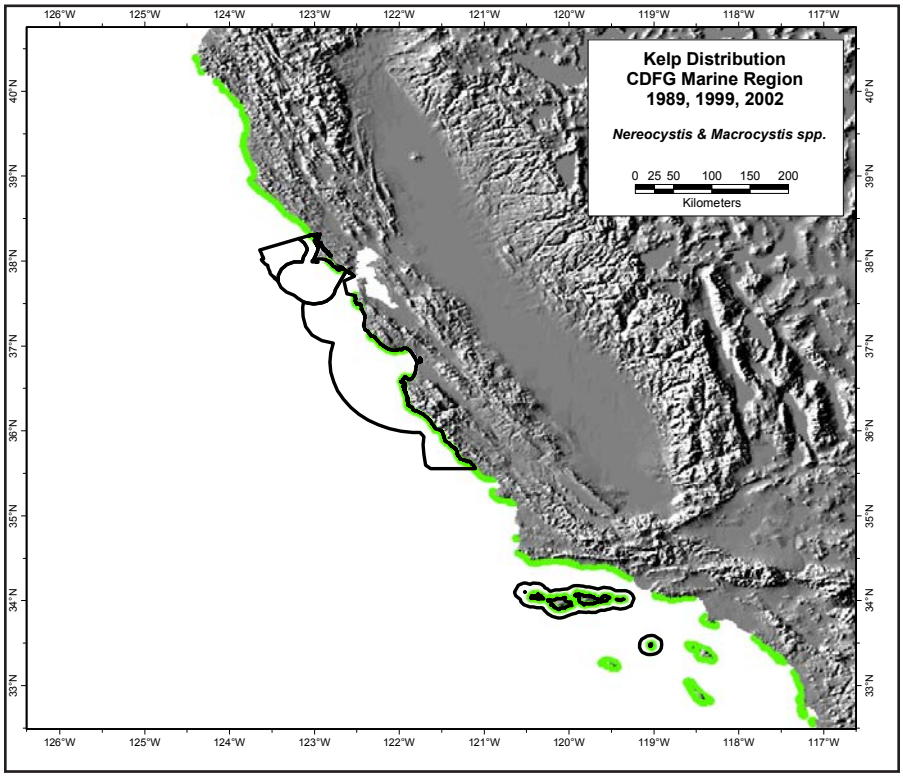

Figure 2.10.1. Kelp distribution based on aerial and multispectral surveys conducted by CDFG during 1989, 1999, and 2002. Kelp polygons have been enlarged for better viewing.

Giant kelp is of significant commercial value in central and southern California, where historically 100,000 tons are harvested annually, most of which comes from southern California (Tarpley, 1992). During the mid 1980's kelp harvesting supported an industry worth $40 million. Few studies examine the potential ecological impacts of intensive and repeated harvesting of kelp. Of these studies performed, results indicate that harvesting does not have a significant effect to kelp abundance and distribution; however, more studies are needed to understand how harvesting affects invertebrate and fish populations (Airamé *et al*., 2003b).

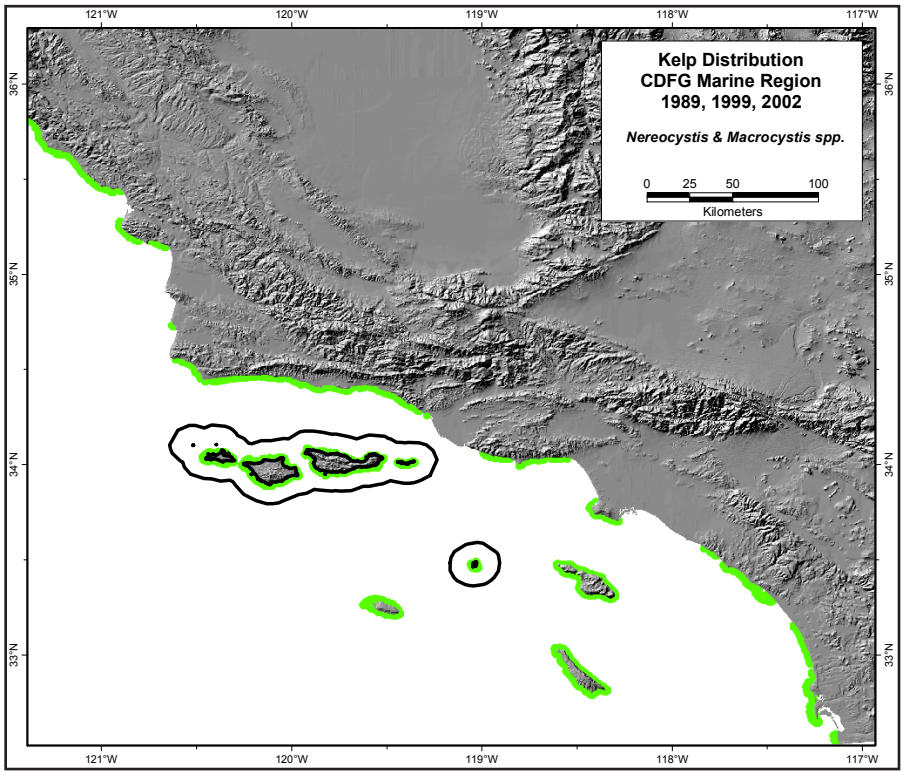

Figure 2.10.2. Kelp distribution off southern California.

Broad-Scale Patterns

Dense forests of kelp grow in rocky nearshore (to 40 m) habitats along the entire California coast (Figure 2.10.1). The GIS kelp data is not segregated by species; however, giant kelp, *Macrocystis pyrifera*, is the predominant species south of Santa Cruz, while bull kelp, *Nereocystis leutkeana*, is more common to the north (Airamé *et al*., 2003a). In central California, kelp beds are typically comprised of narrow bands that parallel the shoreline due to the steepness of the shore. Extensive areas of kelp were found along the shoreline from Cape Mendocino through the Gulf of the Farallones and

Monterey Bay sanctuaries. In southern California extensive kelp beds can extend far offshore along rocky and well stabilized sandy bottoms which have less extreme relief than the region to the north (Miller and Geibel, 1973). Kelp was also broadly distributed in southern California, with large concentrations found from Point Conception to Point Mugu and considerable amounts were contained within the Channel Islands National Marine Sanctuary and southern islands (Figure 2.10.2).

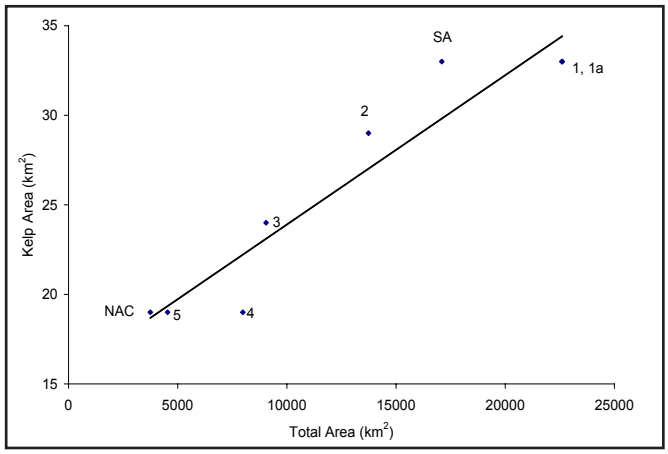

Figure 2.10.3. Regression of kelp area and total area for the current and proposed boundary concepts. Numbers indicate alternatives and NAC=No Action Concept, SA=Study Area.

Analysis of Boundary Concepts

Figure 2.10.2 displays kelp distribution in southern California. Overall, kelp comprised 1% or less of the total area contained within each concept and abundance was significantly greater (r^2=0.90, p>0.0003) within the larger Concepts (1, 1a, 2 and the Study Area) than within Concepts 3, 4, 5 and the NAC (Figure 2.10.3). The OAI was used to compare historic kelp coverage within each boundary concept (Table 2.10.1). Results indicated that the Study Area provided the most favorable gain of kelp habitat, however, this boundary is not considered as a concept. Therefore, Concepts 2 and 3 provide the most benefit in terms of kelp abundance and total area gained relative to the current CINMS boundary.

Summary

- Kelp forests provide habitat that supports many species.
- Patterns of kelp distribution are highly variable and data presented here do not reflect current conditions.
- Results of the OAI suggest that Concept 2 exhibits the greatest benefit among boundary concepts in terms of kelp coverage.

Table 2.10.1. Analysis of kelp distribution within boundary concepts. Numbers in bold indicate an increase in the estimate when compared to the No Action Concept (NAC). OAI estimates shaded in gray represent maximum observed benefit. Delta (Δ) indicates a rate of change calculation, and is always expressed as a percent change from the NAC.

Concept	Area (km²)	High Kelp Area (km²)	Δ Area (%)	Δ Kelp Area (%)	OAI (absolute)
NAC	3475	19.0	-	-	-
5	4538	19.0	21.12	0.00	0.00
4	7981	19.0	113.11	0.00	0.00
3	9044	**24.0**	141.50	26.32	0.19
2	13736	**29.0**	266.78	52.63	0.20
1a	22591	**33.0**	503.23	73.68	0.15
1	22613	**33.0**	503.82	73.68	0.15
SA	*17093*	*33.0*	*356.42*	*73.68*	*0.21*

LITERATURE CITED

Ainley, D.G., W.J. Sydeman, S.A. Hatch, and U.W. Wilson. 1994. Seabird population trends along the west coast of North America: causes and extent of regional concordance. Studies of Avian Biology 15:119-133.

Airamé, S., S. Gaines and C. Caldow. 2003a. Ecological Linkages: Marine and Estuarine Ecosystems of Central and Northern California. NOAA, National Ocean Service. Silver Spring, MD. 164 pp.

Airamé, S., J.E. Dugan, K.D. Lafferty, H. Leslie, D.A. McArdle and R.R. Warner. 2003b. Applying ecological criteria to marine reserve design: a case study from the California Channel Islands. Ecological Applications 13(1):S170-S184.

Allen, S.G. 1994. The distribution and abundance of marine birds and mammals in the Gulf of the Farallones and adjacent waters, 1985-1992. Ph.D. dissertation, University of California, Berkley.

Atkinson, L.P., K.H. Brink, R.E. Davis, B.H. Jones, T. Paluszkiewicz, and D.W. Stuart. 1986. Mesoscale hydrographic variability in the vicinity of Point Conception and Arguello during April-May 1983: The OPUS 1983 Experiment. Journal of Geophysical. Reearch 91:12899-12918.

Auad, G. M.C. Hendershott, and C.D. Winant. 1998. Wind-induced currents and bottom-trapped waves in the Santa Barbara Channel. Journal of Physical Oceanography 28:85-102.

Barth, J.A., S.D. Pierce, and R.L. Smith. 2000. A separating coastal upwelling jet at Cape Blanco, Oregon and its connection to the California Current System. Deep-Sea Research II 47:783-810.

Briggs, K.T., W.M. Breck-Tyler, D.B. Lewis, and D.R. Carlson. 1987. Bird communities ar sea off California: 1975-1983. Studies in Avian Biology 11:1-74.

Channel Islands National Marine Sanctuary (CINMS). 2000. Working Draft Environmental Impact Statement for Channel Islands National Marine Sanctuary: Affected Environment Section. Santa Barbara, CA. 223 pp.

Chelton, D.B. 1984. Seasonal variability of alongshore geostrophic velocity off central California. Journal Geophysical Research 89:3473-3486.

Chelton, D.B., P.A. Bernal, and J.A. McGowan. 1982. Large-scale interannual physical and biological interaction in the California current. Journal of Marine Research 40:1095-1125.

Committe on Environment and Natural Resources (CENR). 2003. An Assessment of Coastal Hypoxia and Eutrophication in U.S. Waters. National Science and Technology Council Committee on Environment and Natural Resources, Washington, D.C.

Collins, C.A., R.G. Paquette and S.R. Ramp. 1996. Annual variability of ocean currents at 350 m depth over the continental slope off Point Sur, California. CalCOFI report 257-263.

Cornuelle, B., T.K. Chereskin, P.P. Niiler, and M.Y. Morris. 2000. Observations and modeling of a California undercurrent eddy. Journal of Geophysical Research 105:1227-1243.

Dailey, M.D., D.J. Reish, and J.W. Anderson. 1993. Ecology of the Southern California Bight: A Synthesis and Interpretation. Berkeley, CA: University of California Press.

Dandonneau, Y., P. Deschamps, J. Nicolas, H. Loisel, J. Blanchot, Y. Montel, F. Thieleux, and G. Bécu. 2003. Seasonal and interannual variability of ocean color and composition of phytoplankton communities in the north Atlantic, equaltorial Pacific, and south Pacific. Unpublished. http://www.lodyc.jussieu.fr/gepco/gepco.html.

Dever, E.P. 2004. Objective maps of near-surface flow states near Point Conception, California. Journal of Physical Oceanography 34(2):444-461.

Engle, J.M. 1979. Ecology and growth of juvenile California spiny lobster, *Panulirus interruptus* (Randall). Ph.D. Dissertation, University of Southern California.

Field, J.M, M.M. Yoklavich, J. DeMarignac, G.M. Cailliet, R.N. Lea, and S.M. Bros. 2002. Small-scale analysis of subtidal fish assemblages and associated habitat characteristics off central California. In Marine Ecolocal Reserves Research Program Results 1996-2001. California Sea Grant Program CD-ROM. LaJolla, CA. 16 pp.

Gabriel, W.L. and A.V. Tyler. 1980. Preliminary analysis of Pacific coast demersal fish assemblages. Marine Fisheries Review 42(3-4):83-88.

Greene, H.G., M.M. Yoklavich, R.M. Starr, V.M. O'Connell, W.W. Wakefield, D.E. Sullivan, J.E. McRea, Jr., and G.M. Cailliet. 1999. A classification scheme for deep seafloor habitats. Oceanoligica Acta 22(6):663-678.

Harms, S. and C.D. Winant. 1998. Characteristic patterns of the circulation in the Santa Barbara Channel. Journal of Geophysical Research 103:3041-3065.

Hendershott, M.C. and C.D. Winant. 1996. Surface circulation in the Santa Barbara Channel. Oceanography 9(2):114-121.

Hickey, B.M. 1979. The California current system – Hypotheses and facts. Progressive Oceanography 8:191-279.

Hickey, B.M. 1993. Physical Oceanography. pp. 19-70. In: M.D. Dailey, D.J. Reish, and J.W. Anderson (Eds.), Ecology of the Southern California Bight: A Synthesis and Interpretation. Berkeley, CA: University of California Press.

Hickey, B. 1998. Coastal Oceanography of Western North America from the Tip of Baja California to Vancouver Island; Coastal Segment. pp. 12947-12966. In:Robinson. A.R. and K.H. Brink (Eds.),The Sea.

Hickey, B.M. 2000. Basin to Basin Water Exchange in the Southern Bight. In: Proceedings of the 5th Channel Islands Symposium. Sponsored by the U.S. Department of Interior Minerals Management Service at the Santa Barbara Museum of Natural History. MMS Pacific OCS Region Document No. 99-0038.

Hixon, M.A., B.N. Tissot, and W.G. Pearcy. 1991. Fish assemblages of rocky banks of the Pacific northwest: final report. Minerals Management Service, MMS 91-0052. Camarillo, CA. 410 pp.

Hixon, M. A. and B. N. Tissot 1992. Fish Assemblages of Rocky Banks of the Pacific Northwest. Final Report Supplement, OCS Study 91-0025, U.S. Minerals Management Service, Camarillo, CA. 128 pp.

Huyer, A., P.M. Kosro, S.J. Lentz, and R.C. Beardsley. 1989. Poleward flow in the California Current System. pp. 142-156 In: Poleward flows along eastern oceanic boundaries, Coastal and Estuarine Studies No. 34. New York, NY: Springer-Verlag Inc.

Jeffrey, C.F.G. 2005. Benthic habitats, fish assemblages, and resource protection in Caribbean marine sanctuaries. PhD. Dissertation, University of Georgia, Athens, GA. 144 pp.

Kaluzny, S.P., S.C. Vega, T.P. Cardoso, and A.A. Shelly. 1998. S+ Spatial Stats: Users manual for Windows and Unix. MathSoft, Inc. Seattle, WA. 316 pp.

Lagerloef, G.S. and R.L. Bernstein. 1988. Empirical orthogonal functional analysis of advanced very high resolution radiometer surface temperature patterns in the Santa Barbara Channel. Journal of Geophysical Research 93:6863-6873.

Leet, W.S., C.M. Dewees, R. Klingbeil, and E.J. Larson (Eds.). 2001. California Living Marine Resources: A Status Report. California Department of Fish and Game. University of California Agriculture and Natural Resources Report SG01-11. 592 pp.

Legendre, P. 1993. Spatial autocorrelation: trouble or new paradigm? Ecology. 74:1659-1673.

Love, M. M. Nishimoto, D. Schroeder, and J. Caselle. 1999. The Ecological Role of Natural Reefs and Oil and Gas Production Platforms on Rocky Reef Fishes in Southern California. Final Interim Report. Minearals Management Service and US Geologic Survey, March, 1999.

Love, M.S., M.M. Yoklavich, and L. Thorsteinson. 2002. The rockfishes of the northeast Pacific. University of California press, Berkley and Los Angeles, CA. 404 pp.

Lynn, R.J. and J.J. Simpson. 1987. The California current system: The seasonal variability of its physical characteristics. Journal of Geophysical Research 92:12947-12966.

Magurran, A.E. 1988. Ecological Diversity and Measurement. Princeton University Press, Princeton, New Jersey.

Matthews, K.R., and L.J. Richards.1991. Rockfish (Scorpaenidae) assemblages of trawlable and untrawlable habitats off Vancouver Island, British Colombia. North American Journal of Fisheries Management 11:312:318.

McGinnis, M.V. 2000. A Recommended Study Site for the CINMS Management Planning Process: Ecological Linkages in the Marine Ecology from Point Sal to Point Mugu, Including the Marine Sanctuary. A Report to the Channel Islands National Marine Sanctuary, NOAA. 50 pp.

Miller, D.J. and J.J. Geibel. 1973. Summary of blue rockfish and lingcod life histories; a reef ecology study; and giant kelp, *Macrocystis pyrifera*, experiments in Monterey Bay, California. California Department of Fish and Game, Fisheries Bulletin 158. 137 pp.

Minerals Management Service (MMS). 1987. Archaeological Resource Study: Morro Bay to Mexican Border (1987). Prepared for the Minerals Management Service, U.S. Department of the Interior by PS Associates, Cardiff, California. OCS Study MMS 87-0025.

NOAA National Centers for Coastal Ocean Science (NCCOS). 2003. A biogeographic assessment off north/central California: To support the joint management plan review for Cordell Bank, Gulf of the Farallones, and Monterey Bay National marine sanctuaries: Phase I – Marine fishes, birds, and mammals. Silver Spring, MD. 145 pp.

National Marine Fisheries Service (NMFS). 2004. Risk Assessment for the Pacific Groundfish FMP. Prepared for the Pacific States Marine Fisheries Commission by MRAG Americas, Inc. Tampa, Florida; TerraLogic GIS, Inc., Stanwood, Washington; NMFS Northwest Fisheries Science Center, FRAM Division, Seattle, Washington; NMFS Northwest Regional Office, Seattle, Washington.

Neander, D.O. 2001. The California Current System: Comparison of Geostrophic Currents, ADCP Currents and Satellite Altimetry. OC3570 Summer Cruise, August 2-5, 2001. http://www.weather.nps.navy.mil/~psguest/OC3570/CDROM/summer2001/Neander/report.pdf

Nishimoto, M.M. and L. Washburn. 2002. Patterns of coastal eddy circulation and abundance of pelagic juvenile fish in the Santa Barbara Channel, California, USA. Marine Ecology Progress Series 241:183-199.

Norris, R.M. and R.W. Webb. 1990. Geology of California. New York, NY: John Wiley and Sons.

O'Reilly, W.C., R.T. Guza and R.J. Seymour. 2000. Wave prediction in the Santa Barbara Channel. In: Proceedings of the 5th Channel Islands Symposium. Sponsored by the U.S. Department of the Interior Minerals Management Service at the Santa Barbara Museum of Natural History. MMS Pacific OCS Region Document No. 99-0038.

Oedekoven, C.S., D.G. Ainley, and L.B. Spear. 2001. Variable responses of seabirds to change in marine climate: California current, 1985-1994. Marine Ecology Progress Series 212:265-281.

Oey, L.Y. 1999. A forcing mechanism for the poleward flow off the southern California coast. Journal of Geophysical Research 104:13529-13539.

Pierce, S.D., R.L. Smith, P.M. Kosro, J.A. Barth and C.D. Wilson. 2000. Continuity of the poleward undercurrent along the eastern boundary of the mid-latitude north Pacific. Deep-Sea Research II 47:811-829.

Reid, J.L. and R.A. Schwartzlose. 1962. Direct measurements of the Davidson Current off central California. Journal of Geophysical Research 67:2491-2497.

San Francisco State University. 2000. http://virga/sfsu.edu/courses/geol1103/2/labs/upwelling/descript1.html (April 20, 2000).

Seapy, R.R. and M.M. Littler. 1980. Biogeography of Rocky Intertidal Macroinvertebrates of the Southern California Islands. pp. 307-323, In: D.M. Power (Ed.), The California Islands: Proceedings of a Multidisciplinary System. Santa Barbara Museum of Natural History, Santa Barbara, CA.

Shannon, E.E. and W. Weaver. 1949. The mathematical theory of communication. University of Illinois Press, Urbana.

Starr, R.M. 1998. Marine harvest refugia for west coast rockfish: A workshop. NOAA-TM-NMFS-SWFSC-255. Pacific Grove, CA. 37 pp.

Stewart, J.G. and B. Myers. 1980. Assemblages of algae and invertebrates in Southern California *Phyllospadix* dominated intertidal habitats. Aquatic Botany 9:73-94.

Strub, P.T. and C. James. 2000. Altimeter-derived variability of surface velocities in the California Current System: 2. Seasonal circulation and eddy statistics. Deep-Sea Research II 47:831-870.

Sullivan, C.M. 1995. Grouping of fishing locations using similarities in species composition for the Moterey Bay area commercial passenger fishing vessel fishery, 1987-1992. California Department of Fish and Game. Marine Resources Technical Report No. 59. Monterey, CA. 37 pp.

Tarpley, J. A,, and D. A. Glantz. 1992. Giant kelp. pp. 2-5. In: W. S. Leet, C. M. Dewees, and C. W. Haugen (Eds.), California's living marine resources and their utilization. California Sea Grant Extension Publication UCSGEP-92-12.

Valle, C.F., J.W. O'Brien, and K.B. Wiese. 1999. Differential habitat use by California halibut, *Paralichthys californicus*, barred sand bass, *Paralabrax nebulifer*, and other juvenile fishes in Alamitos Bay, California. Fisheries Bulletin 97:646-660.

Williams, E.H., and S. Ralston. 2002. Distribution and co-occurrence of rockfishes over trawlable shelf and slope habitats of California and southern Oregon. Fisheries Bulletin 100:836-855.

Yoklavich, M.M., H.G. Greene, G.M. Cailliet, D.E. Sullivan, R.N. Lea, and M.S. Love. 2000. Habitat associations of deep-water rockfishes in a submarine canyon: An example of a natural refuge. Fisheries Bulletin 98:625-641.

Yoklavich, M.M., G.M. Cailliet, R.N. Lea, H.G. Greene, R.M. Starr, J. DeMarignac, and J. Field. 2002. Deepwater habitat and fish resources associated with a marine reserve: implications for fisheries. In: Ecological Reserves Research Program Results 1996-2001. California Sea Grant Program CD-ROM. LaJolla, CA. 63 pp.